Convergent functional effects of antidepressants in major depressive disorder: a neuroimaging meta-analysis

Amin Saberi[1,2,3], Amir Ebneabbasi[4,5], Sama Rahimi[1,2,6], Sara Sarebannejad[7], Zumrut Duygu Sen[8,9,10,11], Heiko Graf[12], Martin Walter[8,9,10,13], Christian Sorg[14,15,16], Julia A. Camilleri[1,2], Angela R. Laird[17], Peter T. Fox[18], Sofie L. Valk[1,2,3], Simon B. Eickhoff[1,2], Masoud Tahmasian[1,2]

[1] Institute of Neurosciences and Medicine (INM-7), Research Centre Jülich, Jülich, Germany.
[2] Institute of Systems Neuroscience, Heinrich Heine University Düsseldorf, Düsseldorf, Germany.
[3] Otto Hahn Research Group for Cognitive Neurogenetics, Max Planck Institute for Human Cognitive and Brain Sciences, Leipzig, Germany
[4] Department of Clinical Neurosciences, University of Cambridge, Biomedical Campus, Cambridge CB2 0QQ, UK.
[5] Cambridge University Hospitals NHS Trust, Cambridge CB2 0SZ, UK.
[6] Neuroscience Center, Goethe University, Frankfurt, Hessen, Germany.
[7] Kavli Institute for Systems Neuroscience, Norwegian University of Science and Technology, Trondheim, Norway.
[8] Department of Psychiatry and Psychotherapy, University Hospital Jena, Jena, Germany.
[9] Clinical Affective Neuroimaging Laboratory (CANLAB), Magdeburg, Germany.
[10] a Éé ~êíã Éå í=ç Ñ=mëó ÅÜ´á~íêó=~å Ç=mëó ÅÜ´çíÜÉê~é ó, University Tübingen, Tübingen, Germany.
[11] German Center for Mental Health, Halle-Jena-Magdeburg, DZP, Germany.
[12] Department of Psychiatry and Psychotherapy III, University of Ulm, Ulm, Germany.
[13] Leibniz Institute for Neurobiology, Brenneckestr. 6, 39118 Magdeburg, Germany.
[14] TUM-Neuroimaging Center (TUM-NIC), Klinikum Rechts der Isar, Technische Universität München, Munich, Germany.
[15] Department of Neuroradiology, Klinikum Rechts der Isar, Technische Universität München, Munich, Germany.
[16] Department of Psychiatry and Psychotherapy, Klinikum Rechts der Isar, Technische Universität München, Munich, Germany.
[17] Department of Physics, Florida International University, Miami, FL, USA.
[18] University of Texas Health Science Center at San Antonio, San Antonio, TX, USA.

*** Corresponding author:** Masoud Tahmasian M.D., Ph.D., Institute of Neuroscience and Medicine, Brain & Behaviour (INM-7), Research Centre Jülich, Wilhelm-Johnen-Straße, Jülich, Germany. Telefon: +49 2461 61-8785, Fax: +49 2461 61-1880. Email: m.tahmasian@fz-juelich.de

Running title: Meta-analytic functional effects of antidepressants in depression

Abstract

Background: Neuroimaging studies have provided valuable insights into the macroscale impacts of antidepressants on brain functions in patients with major depressive disorder. However, the findings of individual studies are inconsistent. Here, we aimed to provide a quantitative synthesis of the literature to identify convergence of the reported findings at both regional and network levels and to examine their associations with neurotransmitter systems.

Methods: Through a comprehensive search in PubMed and Scopus databases, we reviewed 5,258 abstracts and identified 37 eligible functional neuroimaging studies on antidepressant effects in major depressive disorder. Activation likelihood estimation was used to investigate regional convergence of the reported foci of consistent antidepressant effects, followed by functional decoding and connectivity mapping of the convergent clusters. Additionally, utilizing group-averaged data from the Human Connectome Project, we assessed convergent resting-state functional connectivity patterns of the reported foci. Next, we compared the convergent circuit with the circuits targeted by transcranial magnetic stimulation (TMS) therapy. Last, we studied the association of regional and network-level convergence maps with the selected neurotransmitter receptors/transporters maps.

Results: We found regional convergence of the reported treatment-associated increases of functional measures in the left dorsolateral prefrontal cortex, which was associated with working memory and attention behavioral domains. No regional convergence was found across foci of alterations in functional imaging associated with antidepressants. Moreover, we found network-level convergence of functional alterations in a circuit that was prominent in the frontoparietal and salience networks. This circuit was co-aligned with a circuit targeted by anti-subgenual TMS therapy. We observed no significant correlations between our meta-analytic findings with the maps of neurotransmitter receptors/transporters.

Conclusion: Our findings highlight the importance of the left dorsolateral prefrontal cortex, as well as frontoparietal network and the salience network in the therapeutic effects of antidepressants, possibly associated with their role in improving executive functions and emotional processing.

Introduction

Major depressive disorder (MDD) is the most common psychiatric disorder and a leading cause of disability worldwide [1]. Despite decades of research and the development of various pharmacological, psychological, and stimulation-based treatments optimal treatment of MDD remains a challenge [2]. The conventional antidepressant medications, which are the mainstay of MDD treatment, can only achieve clinical response after several weeks of treatment [3] and only in around half the patients [4]. The challenges in the treatment of MDD are partly due to our limited understanding of the mechanisms by which antidepressants interact with the complex and heterogeneous neurobiology of MDD.

First-generation antidepressants were the monoamine oxidase inhibitors (MAOIs) and tricyclic antidepressants (TCAs) which were discovered accidentally, originally intended for treating tuberculosis and schizophrenia [5]. The discovery of the antidepressant effects of these medications, which possess monoaminergic properties, constituted the foundation of the neurotransmitter hypothesis of MDD. This hypothesis postulated that decreased levels of serotonin and norepinephrine in certain brain regions are responsible for depressive symptoms [6]. The neurotransmitter hypothesis of MDD led to the development of other classes of antidepressants, including selective serotonin reuptake inhibitors (SSRIs) and serotonin-norepinephrine reuptake inhibitors (SNRIs), which increase the availability of synaptic monoamine neurotransmitters by inhibiting their reuptake or degradation [5]. While this hypothesis has dominated the field of MDD research and treatment for decades, it is increasingly being questioned, as the supporting evidence for a decreased concentration/activity of serotonin in MDD has been found inconclusive [7]. This, together with the discovery of rapid antidepressant effects of ketamine, a glutamate receptor antagonist [8, 9], suggests that the therapeutic effects of antidepressants cannot be simply explained as rebalancing the synaptic levels of the monoamine neurotransmitters. Thus, it is imperative to study the macroscale effects of antidepressant medications on the brain regions and networks beyond their neurochemical and cellular effects. Understanding these macroscale effects may help in better understanding their clinical effects on various symptoms of MDD which is ultimately needed for improving treatment outcomes.

Neuroimaging techniques such as functional magnetic resonance imaging (fMRI) and positron emission tomography (PET) have been used to study macroscale effects of antidepressants on brain activity, metabolism, or connectivity [10, 11]. However, findings of individual neuroimaging studies have been largely inconsistent, which can be attributed to their methodological and analytic flexibility, center-specific idiosyncrasies, clinical hetero-

geneity of included patients, and the small number of participants, which may make their findings less generalizable and/or reproducible [12, 13]. Neuroimaging meta-analysis is a promising tool to identify the most consistent brain findings by synthesizing the previously published literature [14, 15]. The common approach in neuroimaging meta-analyses, i.e., coordinate-based meta-analysis (CBMA), aims to find potential regional convergence across the peak coordinates of the reported effects in individual studies [16]. Several neuroimaging meta-analyses have previously used this approach to study the regional convergence of the brain effects associated with the treatment of MDD, focusing on various therapeutic approaches and different neuroimaging modalities [17–23]. However, MDD is increasingly being recognized as a brain network disorder with distributed abnormalities across the whole brain, and similarly, the antidepressants' effects could be distributed across the brain rather than localized [10]. Such distributed effects may be overlooked by the CBMA approaches which are inherently intended for regional localization of effects. Recently, a novel meta-analytic approach has been introduced which aims to identify the convergence of reported findings at the level of networks, by characterizing the normative convergent connectivity of the reported foci tested against random foci [24]. Using this approach, it was shown that despite a lack of regional convergence of reported abnormalities in MDD [25], there is a convergence of their connectivity in circuits which recapitulates clinically meaningful models of MDD [24].

Here, we aimed to identify how the findings of the previous functional neuroimaging studies on the effects of antidepressants converge on both regional and network levels by performing an updated CBMA as well as a network-level meta-analysis on the reported findings. Following, we compared our meta-analytic findings with the targets of transcranial magnetic stimulation (TMS) therapy and their associated circuits. Last, we asked whether the pattern of the observed meta-analytic effects of antidepressant medications on functional imaging can be potentially explained by the regional distribution of the neurotransmitter receptors/transporters (NRT) linked to these medications, leveraging the publicly available PET maps of neurotransmitter receptors and transporters [26].

Methods

This meta-analysis was performed according to the best-practice guidelines for neuroimaging meta-analyses [14, 15] and is reported adhering to the Preferred Reporting Items for Systematic Reviews and Meta-Analyses (PRISMA) statement [27]. The protocol for this study

was pre-registered on the International Prospective Register of Systematic Reviews (PROSPERO, CRD42020213202).

Search and study selection

We searched the PubMed and Scopus databases to identify peer-reviewed eligible neuroimaging studies investigating the effects of antidepressants on MDD. The search was performed in July 2022, using the keywords reported in Table S1. In addition, we searched the BrainMap annotated database of neuroimaging experiments using Sleuth by setting the diagnosis to MDD and pharmacology to the antidepressants [28–31]. Further, to avoid missing any additional relevant studies, we traced the references of relevant neuroimaging reviews/meta-analyses. Next, the duplicated records were removed, and the resulting 5258 unique records were assessed for eligibility by two reviewers (S.RJ. and S.SN.) independently. The eligibility of records was assessed first using their titles or abstracts and then, for the potentially relevant records, by examining their full texts. Any disagreements between the reviewers were resolved by another author (A.E. and A.S.).

As suggested previously [14, 15], original studies were included if: 1) they studied patients with MDD, excluding patients with other major psychiatric or neurological comorbidities and adolescent or late-life patients, 2) the patients were treated with antidepressants, 3) the antidepressants effects on the function of gray matter structures were investigated using eligible neuroimaging modalities, i.e., functional magnetic resonance imaging (including task-based [tb-fMRI], resting-state [rs-fMRI] and arterial spin labeling [ASL-fMRI]), fluorodeoxyglucose positron emission tomography (FDG-PET), or single-photon emission computed tomography (SPECT), 4) the results of pre- vs. post-treatment, treated vs. placebo/untreated, or group-by-time interaction contrasts were reported as peak coordinates of significant clusters in standard spaces (Montreal Neurological Institute [MNI] or Talairach) or were provided by the authors at our request, 5) the analysis was performed across the whole brain, was not limited to a region of interest (ROI), and small volume correction (SVC) was not performed, as these approaches are biased toward finding significance in the respective areas, hence violating the assumption of ALE method that all voxels of the brain have a unified chance of being reported [14, 15], and 6) at least six subjects were included in each group (Fig. 1).

Data extraction and preprocessing

From the eligible studies, we extracted demographic and clinical data (number of participants, age, sex, response to treatment, medications, treatment duration), methodological details (imaging modality, scanner field strength, task paradigm, software package, statistical

contrast, and the multiple comparisons correction method), as well as the peak coordinates/foci (x, y, z) of experiments' findings. Of note, we use the term "study" to refer to an individual publication, and the term "experiment" to refer to the individual group-level contrasts reported within each "study" (e.g., Treated > Untreated). Following the data extraction, the coordinates reported in Talairach space were transformed into MNI space [32], so that all the experiments are in the same reference space. If the applied reference space was not explicitly reported or provided by authors after our request, we assumed the default settings of the software packages were used for normalization [14, 15]. In addition, to avoid spurious convergence over the experiments performed on the same/overlapping samples (reported within or across studies), in each meta-analysis, we merged the coordinates from multiple experiments pertaining to the same/overlapping samples, to make sure that each study contributes once per analysis, as suggested previously [14, 15, 33].

Activation likelihood estimation

The revised version of the activation likelihood estimation (ALE) method [16] was used to test the regional convergence of the reported differences against the null hypothesis of randomly distributed findings across the brain. In this method, the peak coordinates are convolved with 3D Gaussian probability distributions that have a full width at half maximum inversely proportional to the sample size. This allows experiments with larger samples to have a greater statistical certainty in the meta-analysis. Next, for each experiment, the convolved foci are combined to generate per-experiment "modeled activation" (MA) maps. Subsequently, the MA maps for all the experiments included in the meta-analysis were combined into an ALE score map, representing the regional convergence of results at each location of the brain. The ALE score map was then statistically tested against a null distribution reflecting randomly distributed findings, to distinguish true convergence from by-chance overlap [16, 33]. Finally, to avoid spurious findings [16], the resulting p-values are corrected for multiple comparisons using the family-wise error correction at the cluster level (cFWE), thresholded at $p < 0.05$.

In addition to an ALE meta-analysis on all included experiments (the 'all-effects' ALE) we performed several complementary ALE meta-analyses based on the direction of the effect (treatment contrast i.e., Treated > Untreated [Tr+] or Untreated > Treated [Tr-]), imaging modality, study design, and type of the antidepressants. The analyses were performed only if a sufficient number of experiments were included in each category, as ALE analyses with too few experiments are likely to be largely driven by a single experiment, and therefore lack sufficient statistical power to provide valid results [34].

Functional decoding of the convergent clusters

We applied the data from task-based functional neuroimaging experiments and their annotated behavioral domains (BD) included in the BrainMap database [28–31] to identify BDs that were significantly associated with the convergent clusters identified in the main ALE analyses [35]. In particular we used binomial tests to assess whether the probability of each cluster activation given a particular BD, i.e., P(Activation|BD), is significantly higher than the overall a priori chance of its activation across all BDs, i.e., P(Activation).

Meta-analytic coactivation mapping of the convergent clusters

We investigated the task-based functional connectivity of the convergent clusters identified in the main ALE analyses using meta-analytic coactivation mapping (MACM) [36]. We used the data from task-based functional neuroimaging experiments on healthy individuals included in the BrainMap database [28–31]. For each identified convergence cluster from the main ALE analyses, we identified all the experiments that reported at least one focus of activation therein, and performed a meta-analysis across those experiments, thresholded at $p < 0.05$ and cFWE-corrected. This approach identifies brain regions that are consistently coactivated with the convergent cluster across all task-based functional neuroimaging experiments.

Resting-state functional connectivity of the convergent clusters

We obtained the group-averaged dense resting-state functional connectivity (RSFC) matrix of the Human Connectome Project (HCP) dataset (n=1003) available in *Cifti* format [37, 38]. The MNI coordinates of the convergent cluster peaks in volumetric space were mapped to their closest 'grayordinate' (cortical vertex or subcortical voxel) in the MNI *Cifti* space based on Euclidean distance. Subsequently, the whole-brain RSFC maps of the foci were extracted from the HCP dense RSFC and were plotted.

Network-based meta-analysis

In addition to the conventional CBMA, we performed network-based meta-analyses [24], to identify convergent connectivity maps of the reported foci compared to randomly distributed foci. We used the normative group-averaged dense RSFC matrix of the HCP dataset in these analyses. For the given set of experiments in the all-effects, Tr+ and Tr- analyses, we first extracted the MNI coordinates of all the reported foci in the included experiments. The MNI coordinates of the foci in volumetric space were then mapped to their closest grayordinate based on Euclidean distance. The foci with no grayordinate in their 10 mm radius were excluded (19 out of 534). Of note, the median distance of the mapped grayordinates from the MNI coordinates of foci was 2.44 mm. Following, the whole-brain

RSFC maps of the foci were extracted from the HCP dense RSFC and averaged to create the RSFC map of the set of experiments. The observed RSFC map was compared to a permutation-based null distribution of RSFC maps to create a z-scored map. Specifically, in each of 1000 permutations we randomly sampled an equal number of foci as reported in the included experiments and averaged their RSFC maps, resulting in a set of 1000 null RSFC maps. Following, we subtracted the mean of the null RSFC maps from the observed RSFC map and divided the result by the standard deviation across the null RSFC maps, to compute the Z-scored RSFC map of the given condition. These maps, referred to as 'convergent connectivity maps', reflect greater- or lower-than-chance connectivity of the reported foci to the rest of the brain, and may indicate circuits affected by antidepressant treatment.

Subsequently, we investigated the distribution of the convergent connectivity maps of each condition across the seven canonical resting-state networks (RSNs). The statistical significance of these associations was assessed using a spin test, which accounts for the spatial autocorrelation in the brain. In this approach, we first calculated the observed mean of convergent connectivity map of a given condition within each RSN, and then tested whether the observed means are more extreme than null means based on 1000 surrogate maps created by randomly spinning the convergent connectivity map on the cortical sphere. The spin surrogate maps were generated as implemented in the *neuromaps* toolbox [39, 40].

Association with transcranial magnetic stimulation targets

We compared the location of the ALE convergent clusters with four TMS target coordinates, including the anatomical 5-CM rule site (MNI -41, 16, 54) [41] and the anti-subgenual site (MNI –38, 44, 26) [42] used in clinical trials as well as the peak sites associated with the clinical improvement of dysphoric symptoms (MNI -32, 44, 34) and anxiosomatic symptoms (MNI -37, 22, 54), as reported previously [43]. In addition, we extracted the RSFC maps of grayordinates corresponding to these coordinates from the HCP dense RSFC and evaluated their spatial correlations with the convergent connectivity maps of antidepressant effects as well as the RSFC maps of ALE convergent clusters by using spin permutation, as described above.

Association of meta-analytic findings with neurotransmitter receptor/transporter densities

The PET maps of tracers associated with NRT were obtained from a previous study [26], which curated these maps from various sources [44–61]. These maps were based on tracers for serotoninergic and noradrenergic receptors/transporters (5HT1a, 5HT1b, 5HT2a, 5HT4, 5HT6, 5HTT, NAT) as well as the NMDA receptor. The PET maps were available in MNI

volumetric space and were parcellated using Schaefer-400 parcellation in the cortex (400 parcels) and Tian S2 parcellation in the subcortex (32 parcels), and were subsequently Z-scored across parcels. In case multiple maps were available for a NRT we calculated an averaged map weighted by the sample size of the source studies.

We then calculated the correlation of parcellated NRT maps with the convergent connectivity maps while accounting for spatial autocorrelation by using variogram-based permutation. In this approach, random surrogate maps were created with variograms that were approximately matched to that of the original map, as implemented in *BrainSMASH* [62]. Furthermore, we used spin permutation to test for over-/underexpression of the NRTs in the ALE convergent clusters. We first rank-normalized the z-scored and parcellated maps of NRTs and after projecting them to the cortical surface, calculated the median rank-normalized density of each NRT within the convergent cluster. Next, we compared the observed median densities against a null distribution calculated based on surrogate NRT maps with preserved spatial autocorrelation. These surrogate maps were created by spinning the parcels on the cortical sphere, as implemented in the *ENIGMA Toolbox* [63]. In all the tests, the resulting p-values were corrected for multiple comparisons across the NRT maps by using false discovery rate (FDR).

Results

Experiments included in the meta-analyses

The study selection process is depicted in Fig. 1. We screened 5258 records resulted from our broad and sensitive search, and assessed 586 full texts for eligibility to finally include 37 studies and 31 experiments with non-overlapping samples (Table 1 and Table S2) [64–100]. Collectively 862 MDD patients were included in the experiments. The patients were treated using SSRIs (n=18), ketamine (n=7), S/NRIs (n=7), mirtazapine (n=2), clomipramine (n=1), amesergide (n=1), quetiapine (n=1), or bupropion (n=1). In seven experiments the patients received variable medications. The imaging modalities included were tb-fMRI (n=18), FDG-PET (n=4), H2O-PET (n=1), rs-fMRI (n=4), ASL-fMRI (n=2) and ^{99m}Tc-HMPAO SPECT (n=3).

Convergent localized effects of antidepressants in the dorsolateral prefrontal cortex

No significant regional convergence was found in our ALE meta-analysis on all the included experiments. Furthermore, the subgroup analyses limited to specific types of treatments or modalities showed no significant convergence (Table 2). However, among the Tr+ experiments (n=21) showing increases in functional imaging measures associated with the treatment, we observed a significant cluster of convergence in the left middle frontal gyrus within the dorsolateral prefrontal cortex (DLPFC) (MNI -38, 30, 28; 129 voxels) (Fig. 2). The convergence in this cluster was driven by contributions from seven experiments [67, 78–81, 83, 85, 99]. The relative contribution of experiments using different medications included SSRIs (58.3%), ketamine (25.4%), and variable classes (16.1%). The contribution of experiments using PET (56.1%) was the highest, followed by fMRI (43.6%) and SPECT (0.3%). The scanning paradigms of contributing experiments included resting state (81.2%) and emotional tasks (18.8%). In the complementary ALE analyses on subgroups of the Tr+ experiments, we observed additional/different clusters of convergence (Fig. S1). The subgroup analysis limited to the 19 Tr+ experiments that only reported pre- versus post-treatment effects revealed clusters in the left (MNI -38, 30, 28; 132 voxels) and right DLPFC (MNI 44, 26, 24; 92 voxels). Similarly, the meta-analysis among Tr+ experiments using treatments other than ketamine (15 experiments) showed clusters of convergence in the left (MNI -38, 30, 30; 95 voxels) and right DLPFC (MNI 44, 26, 24; 106 voxels). The meta-analysis on Tr+ effects reported after more than 4 weeks of treatment (13 experiments) revealed a convergent cluster in the medial superior frontal gyrus (MNI 8, 54, 30; 104 voxels). In the meta-analysis on the Tr+ experiments reporting • 50% rate of clinical response, we found a cluster of convergence in the left supramarginal gyrus (MNI -48, -44, 40; 123 voxels) in addition to the right DLPFC (MNI 44, 26, 24; 123 voxels).

We observed no significant convergence in the ALE meta-analyses performed across Tr- experiments showing decreases of functional imaging features associated with the treatment (22 experiments) as well as their more specific subgroups (Table 2).

Functional decoding and MACM of the dorsolateral prefrontal cortex cluster

Next, we studied the behavioral relevance and connectivity of the convergent cluster identified in the ALE meta-analysis on Tr+ experiments within the left DLPFC. Using the data from BrainMap database we observed that the behavioral domains of working memory (likelihood ratio = 1.85) and attention (likelihood ratio = 1.43) were significantly associated with the activity of this cluster.

The MACM of the left DLPFC cluster showed its significant co-activation with regions in the prefrontal cortex, superior parietal lobule, insula and anterior cingulate and paracingulate cortices ($p_{cFWE} < 0.05$; Fig. 3A). In addition, the RSFC of the left DLPFC cluster center based on the HCP dataset dense connectome showed its connectivity with widespread regions in the prefrontal cortex, superior frontal gyrus, insula, anterior cingulate, paracingulate cortices, supramarginal gyrus, inferior temporal gyrus and basal ganglia, in contrast to its negative resting-state anti-correlation with regions in the subgenual anterior cingulate cortex, orbitofrontal cortex, posterior cingulate, angular gyrus, and temporal pole (Fig. 3B).

Convergent connectivity of antidepressant effects

Having characterized the regional convergence of antidepressant effects using ALE, next, we aimed to investigate meta-analytic effects of antidepressants at a circuit level, following a recently introduced approach [24]. To do so, we used the group-averaged dense functional connectome obtained from the HCP dataset and quantified the convergent connectivity of the reported coordinates of antidepressant effects, which was compared against null connectivity patterns of random points.

The peak coordinates of all the included experiments, indicating alterations in functional imaging measures associated with antidepressants (515 foci from 31 experiments), showed greater-than-chance connectivity of these coordinates with regions in the dorsolateral and medial prefrontal cortex, anterior insula, posterior cingulate cortex, supramarginal gyrus, inferior temporal gyrus, primary visual cortex, and basal ganglia, in contrast to their lower-than-chance connectivity with regions in the subgenual anterior cingulate, posterior cingulate, angular gyrus, temporal pole and superior frontal gyrus (Fig. 4A). We observed significantly higher values of convergent connectivity in the frontoparietal (FPN; $\langle Z \rangle = 4.23$, $p_{spin} < 0.001$) and salience (SAN; $\langle Z \rangle = 3.16$, $p_{spin} = 0.047$) networks (Fig. 4B). Accordingly,

evaluating the distribution of the foci across RSNs revealed significantly higher than chance number of foci in the FPN (n=84, $p_{spin} < 0.001$; Fig. 4B).

The network-level analyses separately performed on the Tr+ (180 foci from 21 experiments) and Tr- effects (206 foci from 22 experiments) revealed convergent connectivity maps which were anti-correlated with each other ($r = -0.45$, $p_{variogram} < 0.001$; Fig. S2A). The convergent connectivity map of the Tr+ effects was significantly more prominent in the FPN ($\langle Z \rangle = 5.41$, $p_{spin} < 0.001$) and default mode network (DMN; $\langle Z \rangle = 1.71$, $p = 0.047$). On the other hand, the convergent connectivity map of Tr- effects was significantly more prominent in the visual (VIS; $\langle Z \rangle = 3.17$, $p_{spin} < 0.001$) and somatomotor (SMN; $\langle Z \rangle = 2.79$, $p_{spin} = 0.016$) networks.

The association of antidepressants effects with TMS targets

The left DLPFC is suggested to be the optimal stimulation target in the TMS treatment of MDD [101, 102]. We next explored whether our meta-analytic findings on the convergent effects of antidepressants might correspond with the different TMS targets. We compared the location of the left DLPFC cluster identified in the Tr+ ALE meta-analysis and observed it was closer to the “anti-subgenual” (14 mm) and “dysphoric” (16 mm) TMS targets than the “5-CM” (29 mm) and “anxiosomatic” (27 mm) targets (Fig. S3A). Moreover, the RSFC map of the Tr+ cluster and the network-level meta-analysis convergent connectivity maps were positively correlated with the RSFC maps of anti-subgenual and dysphoric TMS targets but negatively correlated with the RSFC maps of 5-CM and anxiosomatic stimulation sites (Fig S3B).

The association between neurotransmitter receptor/transporter maps and meta-analytic effects of antidepressants

Lastly, we studied whether the regional and network-level convergence of antidepressant effects colocalizes with the spatial distribution of serotoninergic and noradrenergic NRTs as well as NMDA receptor (Fig. 5a) [26]. We first focused on the cluster of convergence of Tr+ effects in the left DLPFC and quantified the median density of each NRT (rank-normalized) in this region, showing the varying density of the NRTs. However, none of the NRTs were significantly over-/underexpressed in this cluster (Fig. 5b). Next, we evaluated the correlation of parcellated convergent connectivity map with the NRT maps but observed no signifi-

cant correlations (Fig. 5c). Similarly, the NRT maps were not significantly correlated with the parcellated convergent connectivity maps of Tr+ and Tr- experiments (Fig. S4).

Discussion

In the present study, we synthesized findings of the neuroimaging literature on the brain effects associated with pharmacotherapy of MDD at regional and circuit levels. At the regional level, our meta-analysis showed no significant convergence across all the included experiments, though we found convergence of the reported treatment-associated increases of functional measures in the left dorsolateral prefrontal cortex. This convergent cluster was associated with working memory and attention behavioral domains and showed meta-analytical coactivation with regions in the prefrontal cortex, superior parietal lobule and insula. Extending our meta-analysis to the circuit level, we investigated the convergent connectivity of the reported foci and found a circuit that was most prominent in the frontoparietal and salience resting-state functional networks. Following, we found that this circuit was co-aligned with a circuit targeted by anti-subgenual TMS therapy. Last, we studied whether the spatial pattern of the observed regional and network-level meta-analytic effects co-align with the maps of receptors and transporters related to the studied antidepressants and found no significant associations.

Convergent effects of antidepressants on the frontoparietal and salience networks

The pathology in MDD is increasingly thought to be distributed across brain regions and circuits, rather than being localized [10]. In fact, previous ALE meta-analyses aimed at localizing the convergent abnormalities in MDD have revealed minimal or no regional convergence [25, 103, 104]. However, a recent study revisited the functional imaging literature on the brain abnormalities in MDD and, using a connectomic approach, showed that the reported abnormalities in MDD are connected to circuits involving regions such as DLPFC, insula, cingulum, pre-supplementary motor area and precuneus [24]. These circuits were shown to recapitulate clinically meaningful models of MDD, such as a lesion-derived MDD circuit [24]. Here, following a similar approach, we also found network-level convergence of the reported findings in a circuit of brain regions most prominent in the frontoparietal and the salience resting-state networks.

The prominence of the convergent connectivity map in the FPN, together with the convergent cluster found in the ALE meta-analysis on the Tr+ experiments, highlights the

importance of DLPFC and FPN in the therapeutic effects of antidepressants. These regions play pivotal roles in higher executive and cognitive functions of the brain, which are shown to be impaired in patients with MDD [105–108]. More severe deficits of executive functions are linked with higher severity of depressive symptoms [107]. The executive and cognitive dysfunction in MDD is thought to contribute to emotional dysregulation, which is a hallmark of MDD psychopathology [109, 110]. Specifically, patients with MDD might have impairments in cognitive control when processing negative emotions, deficits in the inhibition of mood-incongruent material, and difficulties in attentional disengagement from negative stimuli, which are among the mechanisms that are thought to contribute to emotional dysregulation [109, 110]. Indeed, antidepressants medications are shown to improve the executive functioning of patients with MDD, in the domains of attention and processing speed [111], psychomotor speed [112] and cognitive interference inhibition [108], and can lead to better emotional regulation strategies [113]. Hypoactivity of the prefrontal cortex in MDD is thought to contribute to the deficits of executive functioning [107, 114, 115] and emotional regulation [110, 114, 116, 117]. For instance, patients with MDD have shown a reduced activity of the DLPFC during an attentional interference task using emotional distracters [118], which can be normalized by antidepressants [119]. Furthermore, the FPN in patients with MDD shows reduced within-network connectivity and decreased connectivity with the parietal regions of the dorsal attention network, as reported by a meta-analysis on seed-based RSFC studies [120]. In addition, hypoconnectivity of the FPN with the rest of the brain has been observed in relation to depressive symptoms in the general population [121]. The treatment of MDD using various therapeutic approaches can affect intra- and inter-network connectivity of the FPN [10] with the DMN [122] and SAN [123–125]. The abnormalities of SAN connectivity in MDD include decrease of within-network as well as SAN-FPN connectivity [10, 124, 126]. The SAN consists of regions such as the anterior insula and dorsal anterior cingulate and is involved in guiding behavior in response to salient events and the processing of emotional information and rewards [10, 120, 127]. Accordingly, the deficits in within- and between-network connectivity of SAN is suggested to contribute to the symptoms of depressed mood, anxiety, and anhedonia in MDD [10, 128–130]. Overall, MDD is characterized by altered function and connectivity of distributed networks, importantly including the FPN and SAN, but also the DMN and limbic networks, which can be modulated by the treatment (see review in Chai et al. [10]). Of note, our network-level meta-analysis was performed using resting-state imaging data of healthy subjects, and therefore, provides an indirect view on network-level actions of antidepressants. Further large-scale studies are

needed to investigate these effects using connectomic approaches on MDD patients treated with antidepressants.

Similar networks may be modulated by antidepressants and TMS

We found convergent network-level and regional effects prominent in the FPN and more specifically the DLPFC. The importance of DLPFC and FPN in MDD treatment has further been observed in non-pharmacological therapeutic approaches. Psychotherapy of patients with MDD and PTSD is shown to normalize the activity of DLPFC and increase within-network connectivity of FPN [131]. In addition, the left DLPFC is suggested to be the optimal target of the stimulation in TMS therapy of MDD [101, 102]. High-frequency TMS applied to this region increases its activity, which in turn is thought to have therapeutic effects by modulating the activity of a network of connected regions [41, 101]. A recent retrospective analysis of the clinical effects of the different TMS locations revealed that the improvement in distinct clusters of depressive symptoms, i.e., anxiosomatic and dysphoric symptoms, relates to stimulating targets that engage distinct circuits [43]. Interestingly, we observed that the convergent connectivity map of the antidepressant effects as well as the RSFC map of the left DLPFC cluster were positively correlated with the “dysphoric” peak target circuit and negatively correlated with the circuit of “anxiosomatic” peak target. While the anxiosomatic circuit corresponds to the RSFC map of the anatomical “5 cm” TMS target used in the early clinical trials, the dysphoric cluster circuit resembles that of the more recent connectivity-based “anti-subgenual” TMS targets [42, 43, 101, 102]. The latter circuit is characterized by negative connectivity to sgACC, which was also found in our meta-analytic convergent connectivity map and the RSFC map of the left DLPFC cluster identified in the ALE meta-analysis. Indeed, hyperactivity of the subgenual anterior cingulate cortex in MDD is thought to contribute to increased processing of negative stimuli [115]. Therefore, both the anti-subgenual TMS and antidepressant treatment of MDD might modulate the activity of a similar circuit including DLPFC and sgACC. This circuit, based on the findings from TMS studies, seems to be more effective on dysphoric symptoms [43]. This is particularly interesting given that antidepressant medications have been shown to be more effective for the core emotional symptoms (e.g., sadness) than for sleep and atypical symptoms (e.g., psychomotor agitation) [132]. Future research is needed to more directly address the question of how the brain function changes in association with the effects of antidepressants on the different subsets of depressive symptoms, especially from a meta-analytical perspective.

Lack of association between neurotranmitters and the system-level effects of antidepressants

The neurotransmitter hypothesis of MDD suggests that the dysregulation of the monoaminergic neurotransmitter systems is central to the pathophysiology of MDD, and antidepressants act by normalizing the dysregulations of these neurotransmitter systems [5, 6, 133]. In our analyses, we found that the PET-based maps of serotoninergic and noradrenergic receptors and transporters were not significantly correlated with the regional and network-level meta-analytic effects of antidepressants. This suggests a divergence between the antidepressant effects on brain function, as observed in functional imaging studies, and the regions where their target NRTs are highly expressed. The observed divergence raises the question of what mechanisms may relate the micro-scale actions of antidepressants on the NRTs to their system-level effects on brain function. Molecular imaging techniques combined with functional imaging might provide some clues to this link. The findings of molecular imaging studies in MDD and its treatment are diverse (see a comprehensive review by Ruhé et al. [133]). For example, there has been some evidence of decreased serotonin synthesis rate in the prefrontal and cingulate cortex of patients with MDD [134–136]. However, a recent umbrella review summarizing the research on the serotonin hypothesis of MDD concluded that there is a lack of convincing evidence for the association of MDD with serotoninergic deficits such as a lower serotonin concentration or changes in the receptors [7]. Moreover, the antidepressive effects of ketamine, an NMDA receptor antagonist, highlight the importance of the other, non-monoaminergic neurotransmitters in the pathophysiology and treatment of MDD [8, 9]. These findings have increasingly led to the belief that the monoaminergic neurotransmitter hypothesis of MDD may not provide a full understanding of the disease [7, 137, 138]. However, these neurotransmitter systems are indeed involved in the pathophysiology and treatment of MDD, yet their role needs to be revisited in a broader context. One promising area for future research on this matter is the computational modeling of the changes in brain activity in response to pharmacological interventions using biophysical network models [139] coupled with biological models of neurotransmitter systems [140].

Research in context, strengths, and limitations

The neuroimaging effects of antidepressant treatment in MDD has been previously investigated in a number of CBMAs [17–23] (Table 3). These studies have focused on various types of treatment, with more specific (e.g., only SSRI medications [20]) or broader (e.g., pharmacotherapy, psychotherapy, and ECT [22]) scopes compared to our study. In addition, various

imaging modalities under different conditions have been investigated, from focusing on fMRI experiments during emotional processing tasks [23] to a broader multimodal investigation of the functional and structural imaging experiments [22]. Given the differences in the scope and methodology of the previous CBMAs, it is not unexpected to find that they have reported different meta-analytic findings. However, it is important to note that according to the current guidelines [14, 15], there are a few methodological issues to consider in some of the (earlier) CBMAs which may have influenced their findings. These issues include: i) a small number of experiments included in the main or subgroup analyses, which can limit the power and increase the risk of a single experiment dominating the findings [34], ii) including explicit or hidden ROI-based experiments which are biased to inflate significance in the selected region, iii) using less stringent methods of multiple comparisons correction, e.g., thresholding clusters simply by applying a lenient cluster extent and height, or by using FDR, or iv) performing ALE using the earlier versions of GingerALE (< 2.3.3), in which a software bug was reported that can lead to more lenient multiple comparisons correction [141]. Here, we set out to avoid such methodological issues by following the best-practice guidelines for the CBMAs [14, 15]. Furthermore, we provided network-level accounts of the effects of antidepressants reported in the literature [24], which acknowledges that the effects may be distributed rather than localized, and in doing so, complements the conventional CBMA approach of identifying regional convergence.

Our study had a few limitations as well. The heterogeneity of the included experiments, in terms of imaging modalities, conditions, medications, and the clinical characteristics of the patients, limits our findings, but at the same time, enables identifying convergence of the effects that may be robust to such variability. To identify convergence among more selected, harmonized, subsets of the experiments, we planned subgroup analyses. Yet, it was not possible to perform some of the planned analyses, such as a comparison of different medication classes, due to a limited number of experiments identified in each subgroup. Moreover, here we studied the neuroimaging effects of antidepressant medications on patients with MDD who had been treated but not necessarily responded to the treatment. Of note, in a small subgroup analysis focused on experiments reporting clinical response in at least half the patients, we observed convergent clusters in the left supramarginal gyrus and the right DLPFC (Fig. S1d). It is possible that the neuroimaging effects of antidepressants vary across individual patients, and in turn, relate to their variability in response to treatment. Further original and meta-analytic neuroimaging studies are needed to evaluate the

individual variability of treatment-induced changes in brain function and its relevance to clinical response.

Conclusion

This comprehensive meta-analysis of the functional neuroimaging studies on the regional and network-level convergence of the effects of antidepressant medications in MDD underscores the importance of the FPN (and particularly DLPFC) and SAN in the pharmacotherapy of MDD. This observation may be attributed to the key roles of these regions in executive functions and emotional processing, which may transcend to other therapeutic approaches. In particular, the convergent connectivity map of antidepressant effects engaged a circuit similar to the circuits of TMS targets associated with the improvement of dysphoric symptoms. This may hint at symptoms-specific effects of antidepressants that need to be further investigated in the future. Notably, we identified no associations between our regional and network-level meta-analytic findings with the spatial maps of neurotransmitter receptors/transporters. We highlight the need for future research integrating the multiple levels of antidepressant actions at the micro- and macroscale.

Acknowledgements

AS and SLV were funded by the Max Planck Society (Otto Hahn award) and Helmholtz Association's Initiative and Networking Fund under the Helmholtz International Lab grant agreement InterLabs-0015, and the Canada First Research Excellence Fund (CFREF Competition 2, 2015–2016) awarded to the Healthy Brains, Healthy Lives initiative at McGill University, through the Helmholtz International BigBrain Analytics and Learning Laboratory (HIBALL). SBE was supported by the Deutsche Forschungsgemeinschaft (DFG, EI 816/21-1), the National Institute of Mental Health (R01-MH074457), and the European Union's Horizon 2020 Research and Innovation Programme under Grant Agreement No. 945539 (HBP SGA3).

Conflicts of Interest

The authors declare that the research was conducted in the absence of any commercial or financial relationships that could be construed as a potential conflict of interest.

Data Availability

The coordinates of the foci reported in the included experiments are available in https://doi.org/10.6084/m9.figshare.24592539. The group-averaged dense resting-state functional connectivity matrix from the Human Connectome Project can be accessed at https://db.humanconnectome.org.

References

1. Liu Q, He H, Yang J, Feng X, Zhao F, Lyu J. Changes in the global burden of depression from 1990 to 2017: Findings from the Global Burden of Disease study. J Psychiatr Res. 2020;126:134–140.
2. Cuijpers P, Stringaris A, Wolpert M. Treatment outcomes for depression: challenges and opportunities. Lancet Psychiatry. 2020;7:925–927.
3. de Vries YA, Roest AM, Bos EH, Burgerhof JGM, van Loo HM, de Jonge P. Predicting antidepressant response by monitoring early improvement of individual symptoms of depression: individual patient data meta-analysis. Br J Psychiatry. 2019;214:4–10.
4. Undurraga J, Baldessarini RJ. Randomized, placebo-controlled trials of antidepressants for acute major depression: thirty-year meta-analytic review. Neuropsychopharmacology. 2012;37:851–864.
5. Hillhouse TM, Porter JH. A brief history of the development of antidepressant drugs: from monoamines to glutamate. Exp Clin Psychopharmacol. 2015;23:1–21.
6. Hirschfeld RM. History and evolution of the monoamine hypothesis of depression. J Clin Psychiatry. 2000;61 Suppl 6:4–6.
7. Moncrieff J, Cooper RE, Stockmann T, Amendola S, Hengartner MP, Horowitz MA. The serotonin theory of depression: a systematic umbrella review of the evidence. Mol Psychiatry. 2022:1–14.
8. Coyle CM, Laws KR. The use of ketamine as an antidepressant: a systematic review and meta-analysis. Hum Psychopharmacol. 2015;30:152–163.
9. Demchenko I, Tassone VK, Kennedy SH, Dunlop K, Bhat V. Intrinsic Connectivity Networks of Glutamate-Mediated Antidepressant Response: A Neuroimaging Review. Front Psychiatry. 2022;13:864902.
10. Chai Y, Sheline YI, Oathes DJ, Balderston NL, Rao H, Yu M. Functional connectomics in depression: insights into therapies. Trends in Cognitive Sciences. 2023;27:814–832.
11. Wessa M, Lois G. Brain Functional Effects of Psychopharmacological Treatment in Major Depression: a Focus on Neural Circuitry of Affective Processing. Curr Neuropharmacol. 2015;13:466–479.
12. Botvinik-Nezer R, Holzmeister F, Camerer CF, Dreber A, Huber J, Johannesson M, et al. Variability in the analysis of a single neuroimaging dataset by many teams. Nature. 2020;582:84–88.
13. Poldrack RA, Baker CI, Durnez J, Gorgolewski KJ, Matthews PM, Munafò MR, et al. Scanning the horizon: towards transparent and reproducible neuroimaging research. Nat Rev Neurosci. 2017;18:115–126.
14. Müller VI, Cieslik EC, Laird AR, Fox PT, Radua J, Mataix-Cols D, et al. Ten simple rules for neuroimaging meta-analysis. Neuroscience & Biobehavioral Reviews. 2018;84:151–161.
15. Tahmasian M, Sepehry AA, Samea F, Khodadadifar T, Soltaninejad Z, Javaheripour N, et al. Practical recommendations to conduct a neuroimaging meta-analysis for neuropsychiatric disorders. Hum Brain Mapp. 2019;40:5142–5154.
16. Eickhoff SB, Bzdok D, Laird AR, Kurth F, Fox PT. Activation likelihood estimation meta-analysis revisited. Neuroimage. 2012;59:2349–2361.
17. Boccia M, Piccardi L, Guariglia P. How treatment affects the brain: meta-analysis evidence of neural substrates underpinning drug therapy and psychotherapy in major depression. Brain Imaging Behav. 2016;10:619–627.
18. Chau DT, Fogelman P, Nordanskog P, Drevets WC, Hamilton JP. Distinct Neural-Functional Effects of Treatments With Selective Serotonin Reuptake Inhibitors, Electroconvulsive Therapy, and Transcranial Magnetic Stimulation and Their Relations to

Regional Brain Function in Major Depression: A Meta-analysis. Biol Psychiatry Cogn Neurosci Neuroimaging. 2017;2:318–326.

19. Delaveau P, Jabourian M, Lemogne C, Guionnet S, Bergouignan L, Fossati P. Brain effects of antidepressants in major depression: a meta-analysis of emotional processing studies. J Affect Disord. 2011;130:66–74.
20. Fitzgerald PB, Laird AR, Maller J, Daskalakis ZJ. A meta-analytic study of changes in brain activation in depression. Human Brain Mapping. 2008;29:683–695.
21. Graham J, Salimi-Khorshidi G, Hagan C, Walsh N, Goodyer I, Lennox B, et al. Meta-analytic evidence for neuroimaging models of depression: state or trait? J Affect Disord. 2013;151:423–431.
22. Li C, Hu Q, Zhang D, Hoffstaedter F, Bauer A, Elmenhorst D. Neural correlates of affective control regions induced by common therapeutic strategies in major depressive disorders: an Activation Likelihood Estimation meta-analysis study. Neuroscience & Biobehavioral Reviews. 2022:104643.
23. Ma Y. Neuropsychological mechanism underlying antidepressant effect: a systematic meta-analysis. Mol Psychiatry. 2015;20:311–319.
24. Cash RFH, Müller VI, Fitzgerald PB, Eickhoff SB, Zalesky A. Altered brain activity in unipolar depression unveiled using connectomics. Nat Mental Health. 2023;1:174–185.
25. Müller VI, Cieslik EC, Serbanescu I, Laird AR, Fox PT, Eickhoff SB. Altered Brain Activity in Unipolar Depression Revisited: Meta-analyses of Neuroimaging Studies. JAMA Psychiatry. 2017;74:47–55.
26. Hansen JY, Shafiei G, Markello RD, Smart K, Cox SML, Nørgaard M, et al. Mapping neurotransmitter systems to the structural and functional organization of the human neocortex. Nat Neurosci. 2022;25:1569–1581.
27. Page MJ, McKenzie JE, Bossuyt PM, Boutron I, Hoffmann TC, Mulrow CD, et al. The PRISMA 2020 statement: an updated guideline for reporting systematic reviews. BMJ. 2021;372:n71.
28. Fox PT, Laird AR, Fox SP, Fox PM, Uecker AM, Crank M, et al. BrainMap taxonomy of experimental design: description and evaluation. Hum Brain Mapp. 2005;25:185–198.
29. Fox PT, Lancaster JL. Opinion: Mapping context and content: the BrainMap model. Nat Rev Neurosci. 2002;3:319–321.
30. Laird AR, Lancaster JL, Fox PT. BrainMap: the social evolution of a human brain mapping database. Neuroinformatics. 2005;3:65–78.
31. Vanasse TJ, Fox PM, Barron DS, Robertson M, Eickhoff SB, Lancaster JL, et al. BrainMap VBM: An environment for structural meta-analysis. Hum Brain Mapp. 2018;39:3308–3325.
32. Lancaster JL, Tordesillas-Gutiérrez D, Martinez M, Salinas F, Evans A, Zilles K, et al. Bias between MNI and Talairach coordinates analyzed using the ICBM-152 brain template. Hum Brain Mapp. 2007;28:1194–1205.
33. Turkeltaub PE, Eickhoff SB, Laird AR, Fox M, Wiener M, Fox P. Minimizing within-experiment and within-group effects in Activation Likelihood Estimation meta-analyses. Hum Brain Mapp. 2012;33:1–13.
34. Eickhoff SB, Nichols TE, Laird AR, Hoffstaedter F, Amunts K, Fox PT, et al. Behavior, sensitivity, and power of activation likelihood estimation characterized by massive empirical simulation. Neuroimage. 2016;137:70–85.
35. Müller VI, Cieslik EC, Laird AR, Fox PT, Eickhoff SB. Dysregulated left inferior parietal activity in schizophrenia and depression: functional connectivity and characterization. Front Hum Neurosci. 2013;7:268.
36. Laird AR, Eickhoff SB, Kurth F, Fox PM, Uecker AM, Turner JA, et al. ALE Meta-Analysis Workflows Via the Brainmap Database: Progress Towards A Probabilistic Functional Brain Atlas. Front Neuroinform. 2009;3:23.

37. Glasser MF, Sotiropoulos SN, Wilson JA, Coalson TS, Fischl B, Andersson JL, et al. The minimal preprocessing pipelines for the Human Connectome Project. Neuroimage. 2013;80:105–124.
38. Van Essen DC, Smith SM, Barch DM, Behrens TEJ, Yacoub E, Ugurbil K, et al. The WU-Minn Human Connectome Project: an overview. Neuroimage. 2013;80:62–79.
39. Alexander-Bloch AF, Shou H, Liu S, Satterthwaite TD, Glahn DC, Shinohara RT, et al. On testing for spatial correspondence between maps of human brain structure and function. Neuroimage. 2018;178:540–551.
40. Markello RD, Hansen JY, Liu Z-Q, Bazinet V, Shafiei G, Suárez LE, et al. neuromaps: structural and functional interpretation of brain maps. Nat Methods. 2022;19:1472–1479.
41. Cash RFH, Cocchi L, Lv J, Wu Y, Fitzgerald PB, Zalesky A. Personalized connectivity-guided DLPFC-TMS for depression: Advancing computational feasibility, precision and reproducibility. Hum Brain Mapp. 2021;42:4155–4172.
42. Blumberger DM, Vila-Rodriguez F, Thorpe KE, Feffer K, Noda Y, Giacobbe P, et al. Effectiveness of theta burst versus high-frequency repetitive transcranial magnetic stimulation in patients with depression (THREE-D): a randomised non-inferiority trial. The Lancet. 2018;391:1683–1692.
43. Siddiqi SH, Taylor SF, Cooke D, Pascual-Leone A, George MS, Fox MD. Distinct Symptom-Specific Treatment Targets for Circuit-Based Neuromodulation. American Journal of Psychiatry. 2020:appi.ajp.2019.19090915.
44. Baldassarri SR, Park E, Finnema SJ, Planeta B, Nabulsi N, Najafzadeh S, et al. Inverse changes in raphe and cortical 5-HT1B receptor availability after acute tryptophan depletion in healthy human subjects. Synapse. 2020;74:e22159.
45. Belfort-DeAguiar R, Gallezot J-D, Hwang JJ, Elshafie A, Yeckel CW, Chan O, et al. Noradrenergic Activity in the Human Brain: A Mechanism Supporting the Defense Against Hypoglycemia. J Clin Endocrinol Metab. 2018;103:2244–2252.
46. Beliveau V, Ganz M, Feng L, Ozenne B, Højgaard L, Fisher PM, et al. A High-Resolution In Vivo Atlas of the Human Brain's Serotonin System. J Neurosci. 2017;37:120–128.
47. Ding Y-S, Singhal T, Planeta-Wilson B, Gallezot J-D, Nabulsi N, Labaree D, et al. PET Imaging of the Effects of Age and Cocaine on the Norepinephrine Transporter in the Human Brain Using (S,S)-[11C]O-Methylreboxetine and HRRT. Synapse. 2010;64:30–38.
48. Gallezot J-D, Nabulsi N, Neumeister A, Planeta-Wilson B, Williams WA, Singhal T, et al. Kinetic modeling of the serotonin 5-HT1B receptor radioligand [11C]P943 in humans. J Cereb Blood Flow Metab. 2010;30:196–210.
49. Galovic M, Al-Diwani A, Vivekananda U, Torrealdea F, Erlandsson K, Fryer TD, et al. In vivo NMDA receptor function in people with NMDA receptor antibody encephalitis. 2021:2021.12.04.21267226.
50. Galovic M, Erlandsson K, Fryer TD, Hong YT, Manavaki R, Sari H, et al. Validation of a combined image derived input function and venous sampling approach for the quantification of [18F]GE-179 PET binding in the brain. Neuroimage. 2021;237:118194.
51. Li CR, Potenza MN, Lee DE, Planeta B, Gallezot J-D, Labaree D, et al. Decreased norepinephrine transporter availability in obesity: Positron Emission Tomography imaging with (S,S)-[(11)C]O-methylreboxetine. Neuroimage. 2014;86:306–310.
52. Matuskey D, Bhagwagar Z, Planeta B, Pittman B, Gallezot J-D, Chen J, et al. Reductions in Brain 5-HT1B Receptor Availability in Primarily Cocaine-Dependent Humans. Biol Psychiatry. 2014;76:816–822.
53. McGinnity CJ, Hammers A, Riaño Barros DA, Luthra SK, Jones PA, Trigg W, et al. Initial evaluation of 18F-GE-179, a putative PET Tracer for activated N-methyl D-aspartate receptors. J Nucl Med. 2014;55:423–430.

54. Murrough JW, Czermak C, Henry S, Nabulsi N, Gallezot J-D, Gueorguieva R, et al. The effect of early trauma exposure on serotonin type 1B receptor expression revealed by reduced selective radioligand binding. Arch Gen Psychiatry. 2011;68:892–900.
55. Murrough JW, Henry S, Hu J, Gallezot J-D, Planeta-Wilson B, Neumaier JF, et al. Reduced ventral striatal / ventral pallidal serotonin1B receptor binding potential in major depressive disorder. Psychopharmacology (Berl). 2011;213:547–553.
56. Pittenger C, Adams TG, Gallezot J-D, Crowley MJ, Nabulsi N, James Ropchan null, et al. OCD is associated with an altered association between sensorimotor gating and cortical and subcortical 5-HT1b receptor binding. J Affect Disord. 2016;196:87–96.
57. Radhakrishnan R, Matuskey D, Nabulsi N, Gaiser E, Gallezot J-D, Henry S, et al. In vivo 5-HT6 and 5-HT2A receptor availability in antipsychotic treated schizophrenia patients vs. unmedicated healthy humans measured with [11C]GSK215083 PET. Psychiatry Res Neuroimaging. 2020;295:111007.
58. Radhakrishnan R, Nabulsi N, Gaiser E, Gallezot J-D, Henry S, Planeta B, et al. Age-Related Change in 5-HT6 Receptor Availability in Healthy Male Volunteers Measured with 11C-GSK215083 PET. J Nucl Med. 2018;59:1445–1450.
59. Sanchez-Rangel E, Gallezot J-D, Yeckel CW, Lam W, Belfort-DeAguiar R, Chen M-K, et al. Norepinephrine transporter availability in brown fat is reduced in obesity: a human PET study with [11C] MRB. Int J Obes (Lond). 2020;44:964–967.
60. Saricicek A, Chen J, Planeta B, Ruf B, Subramanyam K, Maloney K, et al. Test-retest reliability of the novel 5-HT1B receptor PET radioligand [11C]P943. Eur J Nucl Med Mol Imaging. 2015;42:468–477.
61. Savli M, Bauer A, Mitterhauser M, Ding Y-S, Hahn A, Kroll T, et al. Normative database of the serotonergic system in healthy subjects using multi-tracer PET. NeuroImage. 2012;63:447–459.
62. Burt JB, Helmer M, Shinn M, Anticevic A, Murray JD. Generative modeling of brain maps with spatial autocorrelation. NeuroImage. 2020;220:117038.
63. Larivière S, Paquola C, Park B, Royer J, Wang Y, Benkarim O, et al. The ENIGMA Toolbox: multiscale neural contextualization of multisite neuroimaging datasets. Nat Methods. 2021;18:698–700.
64. Abdallah CG, Averill LA, Collins KA, Geha P, Schwartz J, Averill C, et al. Ketamine Treatment and Global Brain Connectivity in Major Depression. Neuropsychopharmacology□: Official Publication of the American College of Neuropsychopharmacology. 2017;42:1210–1219.
65. Bremner JD, Vythilingam M, Vermetten E, Charney DS. Effects of antidepressant treatment on neural correlates of emotional and neutral declarative verbal memory in depression. J Affect Disord. 2007;101:99–111.
66. Carlson PJ, Diazgranados N, Nugent AC, Ibrahim L, Luckenbaugh DA, Brutsche N, et al. Neural correlates of rapid antidepressant response to ketamine in treatment-resistant unipolar depression: a preliminary positron emission tomography study. Biological Psychiatry. 2013;73:1213–1221.
67. Cheng Y, Xu J, Arnone D, Nie B, Yu H, Jiang H, et al. Resting-state brain alteration after a single dose of SSRI administration predicts 8-week remission of patients with major depressive disorder. Psychological Medicine. 2017;47:438–450.
68. Downey D, Dutta A, McKie S, Dawson GR, Dourish CT, Craig K, et al. Comparing the actions of lanicemine and ketamine in depression: key role of the anterior cingulate. Eur Neuropsychopharmacol. 2016;26:994–1003.
69. Fonzo GA, Etkin A, Zhang Y, Wu W, Cooper C, Chin-Fatt C, et al. Brain regulation of emotional conflict predicts antidepressant treatment response for depression. Nature Human Behaviour. 2019;3:1319–1331.

70. Frodl T, Scheuerecker J, Schoepf V, Linn J, Koutsouleris N, Bokde ALW, et al. Different effects of mirtazapine and venlafaxine on brain activation: An open randomized controlled fMRI study. Journal of Clinical Psychiatry. 2011;72:448–457.
71. Fu CH, Williams SC, Brammer MJ, Suckling J, Kim J, Cleare AJ, et al. Neural responses to happy facial expressions in major depression following antidepressant treatment. The American Journal of Psychiatry. 2007;164:599–607.
72. Fu CH, Williams SC, Cleare AJ, Brammer MJ, Walsh ND, Kim J, et al. Attenuation of the neural response to sad faces in major depression by antidepressant treatment: a prospective, event-related functional magnetic resonance imaging study. Archives of General Psychiatry. 2004;61:877–889.
73. Fu CHY, Costafreda SG, Sankar A, Adams TM, Rasenick MM, Liu P, et al. Multimodal functional and structural neuroimaging investigation of major depressive disorder following treatment with duloxetine. BMC Psychiatry. 2015;15:82.
74. Gonzalez S, Vasavada MM, Njau S, Sahib AK, Espinoza R, Narr KL, et al. Acute changes in cerebral blood flow after single-infusion ketamine in major depression: A pilot study. Neurology Psychiatry and Brain Research. 2020;38:5–11.
75. Jiang W, Yin Z, Pang Y, Wu F, Kong L, Xu K. Brain functional changes in facial expression recognition in patients with major depressive disorder before and after antidepressant treatment: A functional magnetic resonance imaging study. Neural Regeneration Research. 2012;7:1151–1157.
76. Joe AY, Tielmann T, Bucerius J, Reinhardt MJ, Palmedo H, Maier W, et al. Response-Dependent Differences in Regional Cerebral Blood Flow Changes with Citalopram in Treatment of Major Depression. Journal of Nuclear Medicine. 2006;47:1319–1325.
77. Keedwell P, Drapier D, Surguladze S, Giampietro V, Brammer M, Phillips M. Neural markers of symptomatic improvement during antidepressant therapy in severe depression: subgenual cingulate and visual cortical responses to sad, but not happy, facial stimuli are correlated with changes in symptom score. J Psychopharmacol. 2009;23:775–788.
78. Kennedy SH, Evans KR, Kruger S, Mayberg HS, Meyer JH, McCann S, et al. Changes in regional brain glucose metabolism measured with positron emission tomography after paroxetine treatment of major depression. American Journal of Psychiatry. 2001;158:899–905.
79. Kohn Y, Freedman N, Lester H, Krausz Y, Chisin R, Lerer B, et al. Cerebral perfusion after a 2-year remission in major depression. International Journal of Neuropsychopharmacology. 2008;11:837–843.
80. Komulainen E, Heikkila R, Nummenmaa L, Raij TT, Harmer CJ, Isometsa E, et al. Short-term escitalopram treatment normalizes aberrant self-referential processing in major depressive disorder. Journal of Affective Disorders. 2018;236:222–229.
81. Komulainen E, Glerean E, Heikkilä R, Nummenmaa L, Raij TT, Isometsä E, et al. Escitalopram enhances synchrony of brain responses during emotional narratives in patients with major depressive disorder. Neuroimage. 2021;237:118110.
82. Kraus C, Klöbl M, Tik M, Auer B, Vanicek T, Geissberger N, et al. The pulvinar nucleus and antidepressant treatment: dynamic modeling of antidepressant response and remission with ultra-high field functional MRI. Mol Psychiatry. 2019;24:746–756.
83. Li CT, Chen MH, Lin WC, Hong CJ, Yang BH, Liu RS, et al. The effects of low-dose ketamine on the prefrontal cortex and amygdala in treatment-resistant depression: A randomized controlled study. Human Brain Mapping. 2016;37:1080–1090.
84. Lopez-Sola M, Pujol J, Hernandez-Ribas R, Harrison BJ, Contreras-Rodriguez O, Soriano-Mas C, et al. Effects of Duloxetine Treatment on Brain Response to Painful Stimulation in Major Depressive Disorder. Neuropsychopharmacology. 2010;35:2305–2317.

85. Mayberg HS, Brannan SK, Tekell JL, Silva JA, Mahurin RK, McGinnis S, et al. Regional metabolic effects of fluoxetine in major depression: Serial changes and relationship to clinical response. Biological Psychiatry. 2000;48:830–843.
86. Murrough JW, Collins KA, Fields J, DeWilde KE, Phillips ML, Mathew SJ, et al. Regulation of neural responses to emotion perception by ketamine in individuals with treatment-resistant major depressive disorder. Translational Psychiatry. 2015;5.
87. Reed JL, Nugent AC, Furey ML, Szczepanik JE, Evans JW, Zarate CA. Ketamine normalizes brain activity during emotionally valenced attentional processing in depression. NeuroImage: Clinical. 2018;20:92–101.
88. Reed JL, Nugent AC, Furey ML, Szczepanik JE, Evans JW, Zarate CA. Effects of Ketamine on Brain Activity During Emotional Processing: Differential Findings in Depressed Versus Healthy Control Participants. Biological Psychiatry: Cognitive Neuroscience and Neuroimaging. 2019;4:610–618.
89. Robertson B, Wang L, Diaz MT, Aiello M, Gersing K, Beyer J, et al. Effect of bupropion extended release on negative emotion processing in major depressive disorder: A pilot functional magnetic resonance imaging study. Journal of Clinical Psychiatry. 2007;68:261–267.
90. Rutgen M, Pletti C, Tik M, Kraus C, Pfabigan DM, Sladky R, et al. Antidepressant treatment, not depression, leads to reductions in behavioral and neural responses to pain empathy. Translational Psychiatry. 2019;9.
91. Sankar A, Adams TM, Costafreda SG, Marangell LB, Fu CH. Effects of antidepressant therapy on neural components of verbal working memory in depression. Journal of Psychopharmacology (Oxford, England). 2017;31:1176–1183.
92. Sterpenich V, Vidal S, Hofmeister J, Michalopoulos G, Bancila V, Warrot D, et al. Increased Reactivity of the Mesolimbic Reward System after Ketamine Injection in Patients with Treatment-resistant Major Depressive Disorder. Anesthesiology. 2019;130:923–935.
93. Vlassenko A, Sheline YI, Fischer K, Mintun MA. Cerebral perfusion response to successful treatment of depression with different serotoninergic agents. J Neuropsychiatry Clin Neurosci. 2004;16:360–363.
94. Wagner G, Koch K, Schachtzabel C, Sobanski T, Reichenbach JR, Sauer H, et al. Differential effects of serotonergic and noradrenergic antidepressants on brain activity during a cognitive control task and neurofunctional prediction of treatment outcome in patients with depression. Journal of Psychiatry and Neuroscience. 2010;35:247–257.
95. Walsh ND, Williams SC, Brammer MJ, Bullmore ET, Kim J, Suckling J, et al. A longitudinal functional magnetic resonance imaging study of verbal working memory in depression after antidepressant therapy. Biological Psychiatry. 2007;62:1236–1243.
96. Wang L, Li K, Zhang Q, Zeng Y, Dai W, Su Y, et al. Short-term effects of escitalopram on regional brain function in first-episode drug-naive patients with major depressive disorder assessed by resting-state functional magnetic resonance imaging. Psychological Medicine. 2014;44:1417–1426.
97. Wang L, Li X, Li K, Su Y, Zeng Y, Zhang Q, et al. Mapping the effect of escitalopram treatment on amplitude of low-frequency fluctuations in patients with depression: a resting-state fMRI study. Metabolic Brain Disease. 2017;32:147–154.
98. Wang Y, Xu C, Cao X, Gao Q, Li J, Liu Z, et al. Effects of an antidepressant on neural correlates of emotional processing in patients with major depression. Neuroscience Letters. 2012;527:55–59.
99. Williams RJ, Brown EC, Clark DL, Pike GB, Ramasubbu R. Early post-treatment blood oxygenation level-dependent responses to emotion processing associated with clinical response to pharmacological treatment in major depressive disorder. Brain Behav. 2021;11:e2287.

100. Yin Y, Wang M, Wang Z, Xie C, Zhang H, Zhang H, et al. Decreased cerebral blood flow in the primary motor cortex in major depressive disorder with psychomotor retardation. Prog Neuropsychopharmacol Biol Psychiatry. 2018;81:438–444.
101. Fox MD, Buckner RL, White MP, Greicius MD, Pascual-Leone A. Efficacy of Transcranial Magnetic Stimulation Targets for Depression Is Related to Intrinsic Functional Connectivity with the Subgenual Cingulate. Biological Psychiatry. 2012;72:595–603.
102. O'Reardon JP, Solvason HB, Janicak PG, Sampson S, Isenberg KE, Nahas Z, et al. Efficacy and Safety of Transcranial Magnetic Stimulation in the Acute Treatment of Major Depression: A Multisite Randomized Controlled Trial. Biological Psychiatry. 2007;62:1208–1216.
103. Gray JP, Müller VI, Eickhoff SB, Fox PT. Multimodal Abnormalities of Brain Structure and Function in Major Depressive Disorder: A Meta-Analysis of Neuroimaging Studies. Am J Psychiatry. 2020;177:422–434.
104. Saberi A, Mohammadi E, Zarei M, Eickhoff SB, Tahmasian M. Structural and functional neuroimaging of late-life depression: a coordinate-based meta-analysis. Brain Imaging and Behavior. 2021. 31 July 2021. https://doi.org/10.1007/s11682-021-00494-9.
105. Lee RSC, Hermens DF, Porter MA, Redoblado-Hodge MA. A meta-analysis of cognitive deficits in first-episode Major Depressive Disorder. Journal of Affective Disorders. 2012;140:113–124.
106. Rock PL, Roiser JP, Riedel WJ, Blackwell AD. Cognitive impairment in depression: a systematic review and meta-analysis. Psychological Medicine. 2014;44:2029–2040.
107. Snyder HR. Major depressive disorder is associated with broad impairments on neuropsychological measures of executive function: a meta-analysis and review. Psychol Bull. 2013;139:81–132.
108. Wagner S, Doering B, Helmreich I, Lieb K, Tadi• A. A meta-analysis of executive dysfunctions in unipolar major depressive disorder without psychotic symptoms and their changes during antidepressant treatment. Acta Psychiatr Scand. 2012;125:281–292.
109. Gotlib IH, Joormann J. Cognition and depression: current status and future directions. Annu Rev Clin Psychol. 2010;6:285–312.
110. Joormann J, Stanton CH. Examining emotion regulation in depression: A review and future directions. Behaviour Research and Therapy. 2016;86:35–49.
111. Gudayol-Ferré E, Duarte-Rosas P, Peró-Cebollero M, Guàrdia-Olmos J. The effect of second-generation antidepressant treatment on the attention and mental processing speed of patients with major depressive disorder: A meta-analysis study with structural equation models. Psychiatry Res. 2022;314:114662.
112. Rosenblat JD, Kakar R, McIntyre RS. The Cognitive Effects of Antidepressants in Major Depressive Disorder: A Systematic Review and Meta-Analysis of Randomized Clinical Trials. Int J Neuropsychopharmacol. 2015;19:pyv082.
113. McRae K, Rekshan W, Williams LM, Cooper N, Gross JJ. Effects of antidepressant medication on emotion regulation in depressed patients: an iSPOT-D report. J Affect Disord. 2014;159:127–132.
114. Davidson RJ, Pizzagalli D, Nitschke JB, Putnam K. Depression: perspectives from affective neuroscience. Annu Rev Psychol. 2002;53:545–574.
115. Disner SG, Beevers CG, Haigh EAP, Beck AT. Neural mechanisms of the cognitive model of depression. Nat Rev Neurosci. 2011;12:467–477.
116. Salehinejad MA, Ghanavai E, Rostami R, Nejati V. Cognitive control dysfunction in emotion dysregulation and psychopathology of major depression (MD): Evidence from transcranial brain stimulation of the dorsolateral prefrontal cortex (DLPFC). J Affect Disord. 2017;210:241–248.

117. Ebneabbasi A, Mahdipour M, Nejati V, Li M, Liebe T, Colic L, et al. Emotion processing and regulation in major depressive disorder: A 7T resting-state fMRI study. Hum Brain Mapp. 2021;42:797–810.
118. Fales CL, Barch DM, Rundle MM, Mintun MA, Snyder AZ, Cohen JD, et al. Altered Emotional Interference Processing in Affective and Cognitive-Control Brain Circuitry in Major Depression. Biological Psychiatry. 2008;63:377–384.
119. Fales CL, Barch DM, Rundle MM, Mintun MA, Mathews J, Snyder AZ, et al. Antidepressant treatment normalizes hypoactivity in dorsolateral prefrontal cortex during emotional interference processing in major depression. Journal of Affective Disorders. 2009;112:206–211.
120. Kaiser RH, Andrews-Hanna JR, Wager TD, Pizzagalli DA. Large-Scale Network Dysfunction in Major Depressive Disorder: A Meta-analysis of Resting-State Functional Connectivity. JAMA Psychiatry. 2015;72:603–611.
121. Schultz DH, Ito T, Solomyak LI, Chen RH, Mill RD, Anticevic A, et al. Global connectivity of the fronto-parietal cognitive control network is related to depression symptoms in the general population. Network Neuroscience. 2018;3:107–123.
122. Daws RE, Timmermann C, Giribaldi B, Sexton JD, Wall MB, Erritzoe D, et al. Increased global integration in the brain after psilocybin therapy for depression. Nat Med. 2022;28:844–851.
123. Fischer AS, Holt-Gosselin B, Fleming SL, Hack LM, Ball TM, Schatzberg AF, et al. Intrinsic reward circuit connectivity profiles underlying symptom and quality of life outcomes following antidepressant medication: a report from the iSPOT-D trial. Neuropsychopharmacol. 2021;46:809–819.
124. Liu J, Fan Y, Ling-Li Zeng, Liu B, Ju Y, Wang M, et al. The neuroprogressive nature of major depressive disorder: evidence from an intrinsic connectome analysis. Transl Psychiatry. 2021;11:1–11.
125. Mkrtchian A, Evans JW, Kraus C, Yuan P, Kadriu B, Nugent AC, et al. Ketamine modulates fronto-striatal circuitry in depressed and healthy individuals. Mol Psychiatry. 2021;26:3292–3301.
126. Sha Z, Wager TD, Mechelli A, He Y. Common Dysfunction of Large-Scale Neurocognitive Networks Across Psychiatric Disorders. Biological Psychiatry. 2019;85:379–388.
127. Seeley WW, Menon V, Schatzberg AF, Keller J, Glover GH, Kenna H, et al. Dissociable Intrinsic Connectivity Networks for Salience Processing and Executive Control. J Neurosci. 2007;27:2349–2356.
128. Gunning FM, Oberlin LE, Schier M, Victoria LW. Brain-based Mechanisms of Late-Life Depression: Implications for Novel Interventions. Semin Cell Dev Biol. 2021;116:169–179.
129. Yuan H, Zhu X, Tang W, Cai Y, Shi S, Luo Q. Connectivity between the anterior insula and dorsolateral prefrontal cortex links early symptom improvement to treatment response. Journal of Affective Disorders. 2020;260:490–497.
130. Quevedo K, Ng R, Scott H, Kodavaganti S, Smyda G, Diwadkar V, et al. Ventral Striatum Functional Connectivity during Rewards and Losses and Symptomatology in Depressed Patients. Biological Psychology. 2017;123:62–73.
131. Yang Z, Oathes DJ, Linn KA, Bruce SE, Satterthwaite TD, Cook PA, et al. Cognitive Behavioral Therapy Is Associated With Enhanced Cognitive Control Network Activity in Major Depression and Posttraumatic Stress Disorder. Biol Psychiatry Cogn Neurosci Neuroimaging. 2018;3:311–319.
132. Chekroud AM, Gueorguieva R, Krumholz HM, Trivedi MH, Krystal JH, McCarthy G. Reevaluating the Efficacy and Predictability of Antidepressant Treatments. JAMA Psychiatry. 2017;74:370–378.
133. Ruhé HG, Frokjaer VG, Haarman B (Benno) CM, Jacobs GE, Booij J. Molecular Imaging of Depressive Disorders. In: Dierckx RAJO, Otte A, de Vries EFJ, van Waarde A,

Sommer IE, editors. PET and SPECT in Psychiatry, Cham: Springer International Publishing; 2021. p. 85–207.

134. Rosa-Neto P, Diksic M, Okazawa H, Leyton M, Ghadirian N, Mzengeza S, et al. Measurement of brain regional alpha-[11C]methyl-L-tryptophan trapping as a measure of serotonin synthesis in medication-free patients with major depression. Arch Gen Psychiatry. 2004;61:556–563.
135. Agren H, Reibring L. PET studies of presynaptic monoamine metabolism in depressed patients and healthy volunteers. Pharmacopsychiatry. 1994;27:2–6.
136. Agren H, Reibring L, Hartvig P, Tedroff J, Bjurling P, Hörnfeldt K, et al. Low brain uptake of L-[11C]5-hydroxytryptophan in major depression: a positron emission tomography study on patients and healthy volunteers. Acta Psychiatr Scand. 1991;83:449–455.
137. Hindmarch I. Beyond the monoamine hypothesis: mechanisms, molecules and methods. Eur Psychiatry. 2002;17 Suppl 3:294–299.
138. Taylor C, Fricker AD, Devi LA, Gomes I. Mechanisms of action of antidepressants: from neurotransmitter systems to signaling pathways. Cell Signal. 2005;17:549–557.
139. Deco G, Cruzat J, Cabral J, Knudsen GM, Carhart-Harris RL, Whybrow PC, et al. Whole-Brain Multimodal Neuroimaging Model Using Serotonin Receptor Maps Explains Non-linear Functional Effects of LSD. Curr Biol. 2018;28:3065-3074.e6.
140. Kringelbach ML, Cruzat J, Cabral J, Knudsen GM, Carhart-Harris R, Whybrow PC, et al. Dynamic coupling of whole-brain neuronal and neurotransmitter systems. Proceedings of the National Academy of Sciences. 2020;117:9566–9576.
141. Eickhoff SB, Laird AR, Fox PM, Lancaster JL, Fox PT. Implementation errors in the GingerALE Software: Description and recommendations. Hum Brain Mapp. 2017;38:7–11.

Figure Legends

Fig. 1. Study selection flowchart.
MDD: major depressive disorder, LLD: late-life depression, ROI: region of interest, SVC: small volume correction.

Fig. 2. Treatment-induced increase of voxel-based physiology in the left middle frontal gyrus. A. Peak coordinates of the included experiments in Treated > Untreated (red) and Untreated > Treated (blue) comparisons. Each dot represents a peak coordinate. B. Activation likelihood estimation showed significant convergence of Treated>Untreated comparisons in the left dorsolateral prefrontal cortex (DLPFC) after family-wise error correction at cluster level.

Fig. 3. Connectivity mapping of the left dorsolateral prefrontal cortex cluster. Using the center of convergent cluster at the left dorsolateral prefrontal cortex as the seed (outlined patch), the meta-analytical co-activation (A) and resting-state functional connectivity (B) maps are shown.

Fig. 4. Network-level convergence of antidepressant effects. A. The cortical and subcortical map (left) represent z-scored convergent connectivity map of the foci from all experiments. The distribution of convergent connectivity map across the resting-state networks (RSNs) is shown (right). Asterisk denotes networks with mean convergent connectivity significantly more extreme than a null distribution based on surrogate spun maps. B. The radar plot (left) shows the number of foci in each RSN. Asterisk denotes networks with statistically significant counts of observed foci compared to a null based on random foci.
VIS: visual network, SMN: somatomotor network, DAN: dorsal attention network, SAN: salience network, LIM: limbic network, FPN: frontoparietal network, DMN: default mode network.

Fig. 5. Association of meta-analytic findings with neurotransmitter receptor/transporter maps. A. The parcellated and z-scored PET maps of neurotransmitter receptor/transporter (NRT) are shown. Red outline indicates the left dorsolateral prefrontal cortex (L DLPFC) convergent cluster. B. Median rank-normalized density of NRTs in L DLPFC cluster. **C.** Correlation of parcellated convergent connectivity map with the PET maps.

Table 1. Characteristics of studies included in this meta-analysis

#	First Author, Year [a]	N (female %) Treated / Untreated	Responded %	Age Treated / Untreated	Wash out period	Antidepressant medication	Duration between Scans	Modality
1	Abdallah, C. G., 2017	18 (44%)	55.5%	43	1 w	Ketamine	1 d	rs-fMRI (GBC)
	Murrough, J. W., 2015							tb-fMRI
2	Bremner, J. D., 2007	13 (84%)	100%	40.0[c]	4 w	Fluoxetine or Venlafaxine	6 +/- 3 m	H_2O-PET
3	Carlson, P. J., 2013	20 (30%)	30.0%	48	2 w	Ketamine	1-3 d	FDG-PET
4	Cheng, Y., 2017	38 (70%[c])	60%	28[c]	Drug-naive	Escitalopram	5 h, 4 w, 8 w	rs-fMRI (fALFF)
5	Downey, D., 2016	21 (62%) / 19 (58%)	NR	27.1 / 25.7	NR	Ketamine	45 min	rs-fMRI
6	Fonzo, G. A., 2019	96 (72%) / 105 (64%)	NR	37 / 36	NR	Sertraline	8 w	tb-fMRI
7	Frodl, T., 2011	24 (33%)	NR	39	1 y	Venlafaxine or Mirtazapine	4 w	tb-fMRI
8	Fu, C. H., 2004, 2007	19 (68%)	NR	43	NR	Fluoxetine	8 w	tb-fMRI
9	Fu, C. H., 2015	24 (41%[c])	79%	40.2	4 weeks	Duloxetine	12 w	tb-fMRI
10	Gonzalez, S., 2020	11 (27%)	45.4%	48	None	Ketamine	1 h, 6 h, 24 h	ASL-fMRI
11	Jiang, W., 2012	21 (57%)	100%	29	Drug-naive	Escitalopram	8-12 w	tb-fMRI
12	Joe, A.Y., 2006	35 (72%)	53.8%	45.3	NR	Citalopram	3 w	^{99m}Tc-HMPAO SPECT
13	Keedwell, P., 2008	12 (50%)	66%	49.0	Drug-naive	Variable	6 – 18 w	tb-fMRI

14	Kennedy, S. H., 2001	13 (0%)	100%	37	4 w	Paroxetine	6 w	FDG-PET
15	Kohn, Y., 2008	11 (54%)	100%	49	Variable	Paroxetine, Fluoxetine or Clomipramine	2 y	^{99m}Tc-HMPAO SPECT
16	Komulainen, E., 2018	17 (53%) / 15 (60%)	NR	27 / 23	4 m	Escitalopram	1 w	tb-fMRI
	Komulainen, E., 2021	15 (53%) / 14 (57%)	NR	29 / 24	NR			
17	Kraus, C., 2019	26 (73%) / 36 (63%)	84%	30.4 / 28.5	3 m	Escitalopram ± Ven-lafaxine or Mitrazapine	12 w	tb-fMRI
	Rütgen, M., 2019	29 (72%)	75.8%	30	3 m			
18	Li, C. T., 2016	32 (69%)	31.2%	44	NR	Ketamine	1 h	FDG-PET
19	Lopez-Sola, M., 2010	13 (85%)	69.2%	45	15 d	Duloxetine	1 w, 8 w	tb-fMRI
20	Mayberg, H. S., 2000	10 (0%)	50.0%	49[c]	1 m	Fluoxetine	1 w, 6 w	FDG-PET
21	Reed, J. L., 2018, 2019	28 (64%[c])	NR	36[c]	2 w	Ketamine	2d, 11d	tb-fMRI
22	Robertson, B., 2007	8 (75%)	75%	41[c]	NR	Bupropion	8 w	tb-fMRI
23	Sankar, A., 2017	23 (56%)	78.2%	40	4 w	Duloxetine	12 w	tb-fMRI
24	Sterpenich, V., 2019	10 (60%)	NR	51	None	Ketamine	1 d, 7 d	tb-fMRI
25	Vlassenko, A., 2004	14 (57%)	100%	43.1	3 w	Fluoxetine, Paroxetine or Amesergide	12 w	^{99m}Tc-HMPAO SPECT
26	Wagner, G., 2010	20 (90%)	50.0%	39	Variable	Citalopram or Reboxetine	6 w	tb-fMRI
27	Walsh, N. D., 2007	20 (70%)	75.0%	44	NR	Fluoxetine	8 w	tb-fMRI
28	Wang, L., 2014	14 (36%)	100%	33	Drug-naive	Escitalopram	8 w	rs-fMRI (ReHo)

	Wang, L., 2017	20 (55%)	100%	35				rs-fMRI (fALFF)
29	Wang, Y., 2012	18 (61%)	NR	32	Drug-naive	Fluoxetine	8 w	tb-fMRI
30	Williams, R. J., 2021	38 (68%)	57% (after 8 weeks)	36.2	NR	Citalopram or Quetiap-ine	1 w	tb-fMRI
31	Yin, Y., 2018	11 (36%)	100%	49.2	4 w	Variable	8 w	ASL-fMRI

[a] Publications with overlapping samples are grouped together, [b] Mean or median, [c] Reported for all the subjects rather than those in the included experiment

NR: not reported, SSRI: selective serotonin reuptake inhibitor, SNRI: serotonin-norepinephrine reuptake inhibitor, NRI: norepinephrine reuptake inhibitor, NMDAR: N-methyl-D-aspartate receptor, NDRI: fMRI: functional magnetic resonance imaging, rs-fMRI: resting state fMRI, tb-fMRI: task based fMRI, ASL-fMRI: arterial spin labeling fMRI, FDG-PET: fluorodeoxyglucose-positron emission tomography, SPECT: single-photon emission computed tomography, GBC: global brain connectivity, fALFF: fractional amplitude of low-frequency fluctuations, ReHo: regional homogeneity, ASL: arterial spin labeling.

Table 2. Activation Likelihood Estimation (ALE) analyses on the effects of antidepressants in major depressive disorder

Experiments	Comparison	N	Min p_{cFWE}[a]	Convergence
All	All	31	0.402	-
	Treated > Untreated	21	**0.007**	L DLPFC
	Treated < Untreated	22	0.624	-
Based on modality				
Rest	All	13	0.056	-
Task	All	19	0.970	-
Based on treatment and clinical setting				
Excluding ketamine	All	24	0.505	-
	Treated > Untreated	15	**0.024**	L DLPFC, R DLPFC
	Treated < Untreated	17	0.475	-
Pre- versus post-treatment effects	All	25	0.323	-
	Treated > Untreated	19	**0.005**	L DLPFC, R DLPFC
	Treated < Untreated	21	0.482	-
Treatment duration > 4 weeks	All	21	0.352	-
	Treated > Untreated	13	**0.014**	R mSFG
	Treated < Untreated	15	0.197	-
Response in •50% of subjects	All	20	0.636	-
	Treated > Untreated	13	**0.009**	L SMG, R DLPFC
	Treated < Untreated	16	0.371	-

[a] Bold p-values indicate statistical significance.

cFWE: cluster-wise family-wise error, SSRI: selective serotonin reuptake inhibitor, L: left, R: right, DLPFC: dorsolateral prefrontal cortex, mSFG: medial superior frontal gyrus, SMG: supramarginal gyrus.

Table 3. Comparison of the existing coordinate-based neuroimaging meta-analyses on the brain effects of antidepressants.

CBMA	N studies[a]	Treatment	Imaging	Method	Findings
Fitzgerald et al., 2008	9	SSRI	PET, SPECT (resting state)	ALE, FDR-corrected, BrainMap	↑: middle frontal gyrus, inferior frontal gyrus, anterior cingulate cortex, precentral gyrus, supramarginal gyrus, posterior cingulate gyrus, inferior parietal lobe, mid-brain, putamen ↓: middle and superior frontal gyri, medial frontal gyrus, subgenual and pregenual anterior cingulate, parahippocampal gyrus, hippocampus, insula, putamen
Delaveau et al., 2011	9	Antidepres-sants	fMRI, PET (emotional activation)	ALE, FDR-corrected, GingerALE 2.0	↑: dorsal medial prefrontal cortex, dorsolateral prefrontal cortex, cuneus, fusiform gyrus, lingual gyrus, middle temporal gyrus, putamen, caudate, thalamus, anterior insula, anterior cingulate cortex ↓: thalamus, caudate, putamen, globus pallidus, hippo-campus, amygdala, parahippocampal gyrus, anterior insula, anterior cingulate cortex, orbitofrontal cortex, posterior cingulate cortex, middle frontal gyrus,

					pre / postcentral gyri, lingual gyrus, cerebellum, supramarginal gyrus, fusiform gyrus
Graham et al., 2013	4	Any	fMRI	ALE / GPR, FDR-corrected, GingerALE 2.1 / custom code	↑: - (ALE), precentral gyrus, precuneus, dorsolateral prefrontal cortex (GPR) ↓: superior temporal gyrus, cerebellum (ALE), precuneus, dorsal lateral prefrontal cortex, lateral occipital region (GPR)
Ma, 2015 [b]	22	SSRI, SNRI	fMRI (emotional processing)	ALE, FDR-corrected, GingerALE 2.3	↑: dorsolateral prefrontal cortex (negative emotions) ↓: amygdala, hypothalamus, putamen, middle temporal gyrus, ventromedial prefrontal cortex, posterior insula, middle frontal gyrus (negative emotions) ↑↓: amygdala, dorsolateral prefrontal cortex, hippocampus, ventromedial prefrontal cortex, anterior cingulate cortex, fusiform, anterior insula, precuneus (positive emotions)
Boccia et al., 2016	12	Antidepressants, Psychotherapy	fMRI	ALE, FDR-corrected, GingerALE 2.1	↑↓: insula, anterior cingulate cortex, precentral and postcentral gyri, middle frontal gyrus, precuneus, basal ganglia, putamen, cerebellum
Chau et al., 2017	7	SSRI, TMS, ECT	PET, SPECT, ASL-fMRI (resting	MLKD, cFWE-corrected	↑: - ↓: anterior insula

			state)		
Li et al., 2022[c]	33	Antidepressants (incl. ketamine), CBT, ECT	fMRI, PET, VBM	ALE, cFWE-corrected, GingerALE 3.0	↑: amygdala, parahippocampal gyrus, thalamus ↑↓: amygdala, parahippocampal gyrus, thalamus, anterior cingulate cortex, middle frontal gyrus, insula, claustrum
Current paper	37	Antidepressants (incl. ketamine)	fMRI, PET, SPECT	ALE, cFWE-corrected, pyALE	↑: dorsolateral prefrontal cortex ↓: - ↑↓: -

[a] Only includes number of studies on the effects of pharmacotherapy on MDD, excluding other treatments and disorders, [b] Reported results indicate antidepressant effects in mood disorders including depression and anxiety. Results specific to MDD were not reported. [c] Reported results indicate effects of all treatments. Specific effects of antidepressant medications were not reported.

↑: increased imaging measures, ↓: decreased imaging measures, ↑↓: changed imaging measure in any direction , SSRI: selective serotonin reuptake inhibitor, SNRI: serotonin-norepinephrine reuptake inhibitor, TMS: transcranial magnetic stimulation, CBT: cognitive behavioral therapy ECT: electroconvulsive therapy, PET: positron emission tomography, SPECT: single-photon emission computed tomography, fMRI: functional magnetic resonance imaging, ASL: arterial spin labeling, VBM: voxel-based morphometry, ALE: activation likelihood estimation, FDR: false discovery rate, MKLD: cFWE: cluster-level family-wise error correction, multilevel kernel density.

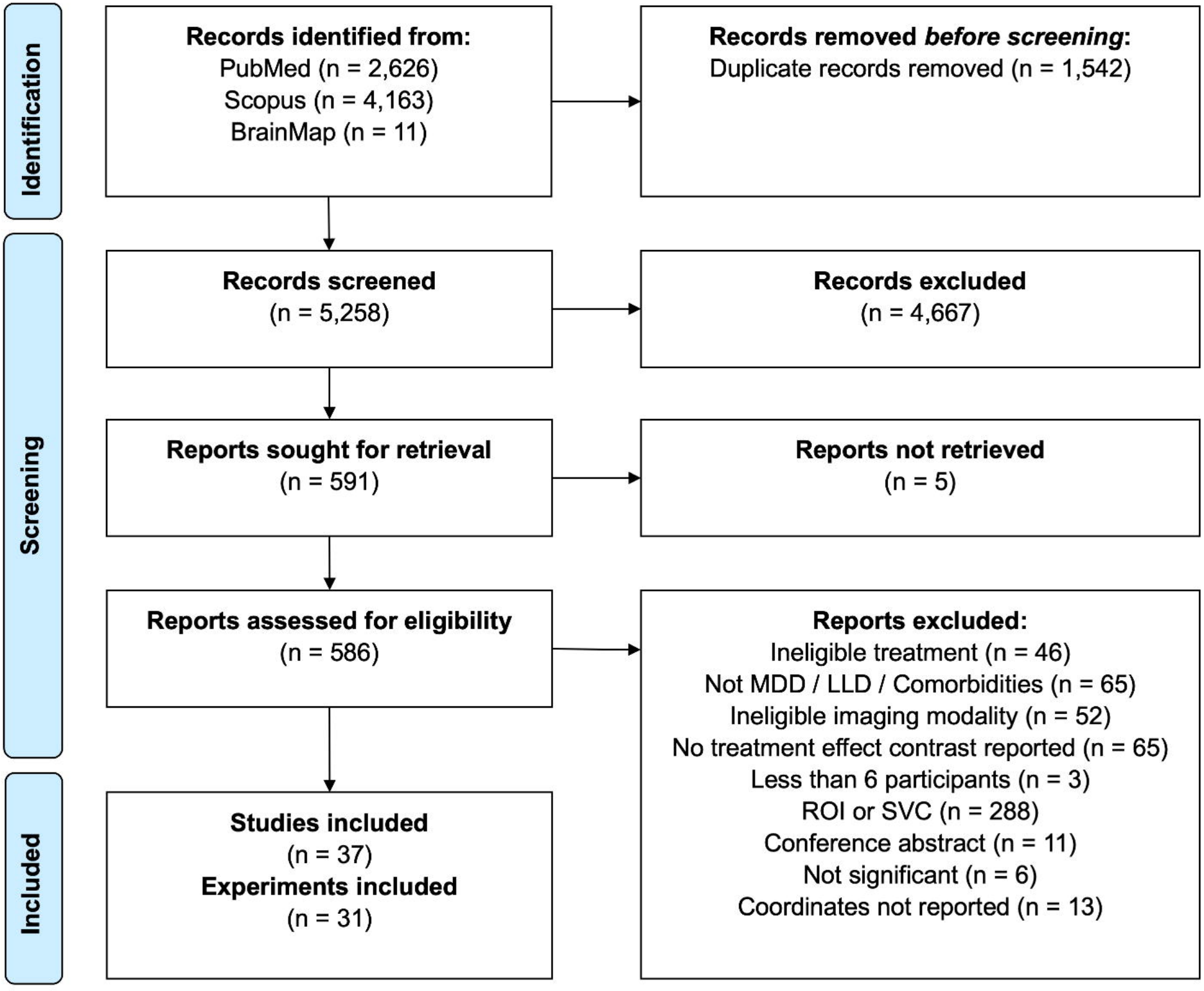
Identification
Screening
Included
Records identified from:
PubMed (n = 2,626)
Scopus (n = 4,163)
BrainMap (n = 11)
Records removed *before screening*:
Duplicate records removed (n = 1,542)
Records screened
(n = 5,258)
Records excluded
(n = 4,667)
Reports sought for retrieval
(n = 591)
Reports not retrieved
(n = 5)
Reports assessed for eligibility
(n = 586)
Reports excluded:
Ineligible treatment (n = 46)
Not MDD / LLD / Comorbidities (n = 65)
Ineligible imaging modality (n = 52)
No treatment effect contrast reported (n = 65)
Less than 6 participants (n = 3)
ROI or SVC (n = 288)
Conference abstract (n = 11)
Not significant (n = 6)
Coordinates not reported (n = 13)
Studies included
(n = 37)
Experiments included
(n = 31)

A. Peak coordinates of antidepressant effects

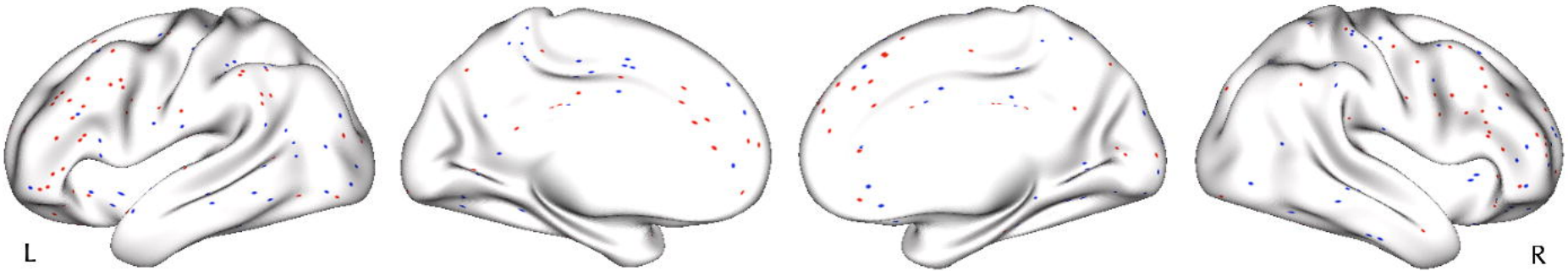

B. Activation likelihood estimation
(Treated > Untreated)

Treated > Untreated
Untreated > Treated

A. Meta-analytical coactivation

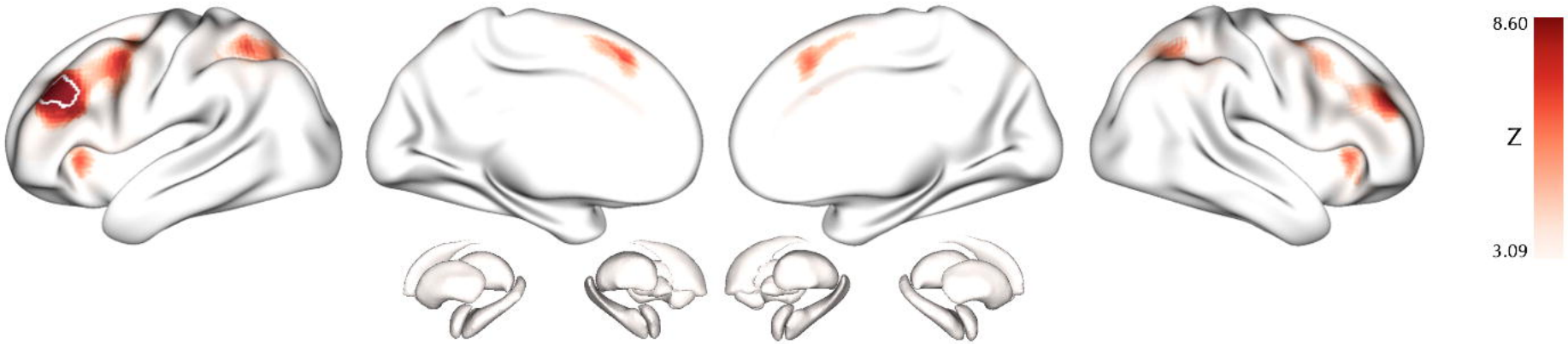

B. Resting-state functional connectivity

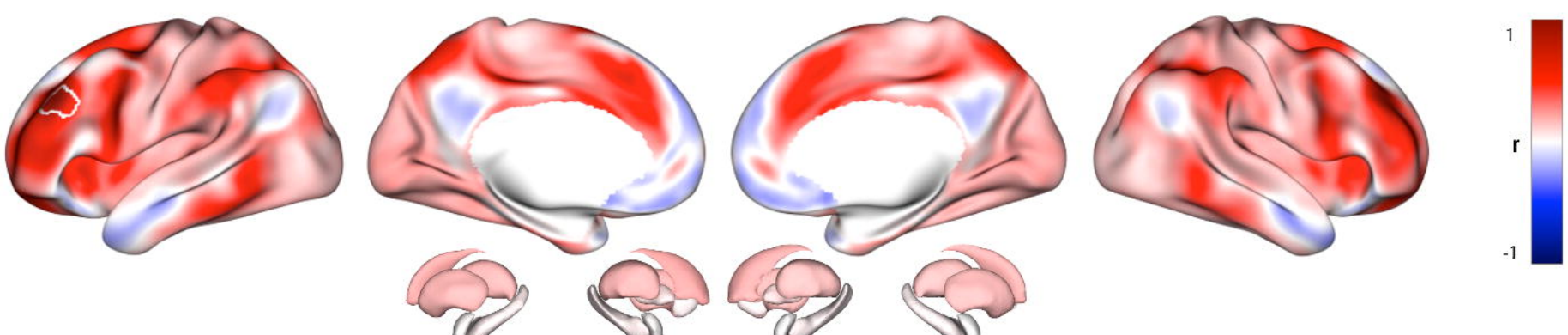

A. Convergent connectivity map of foci

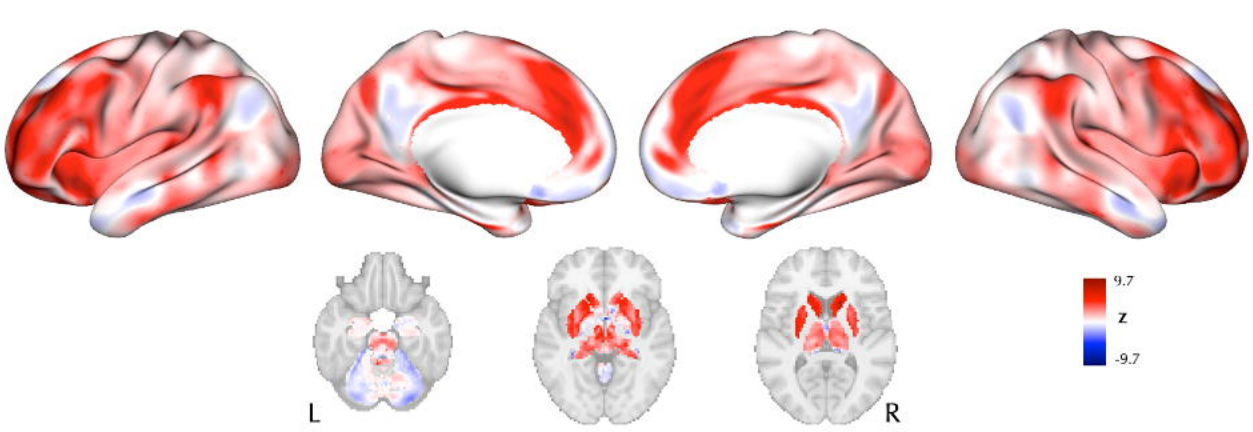

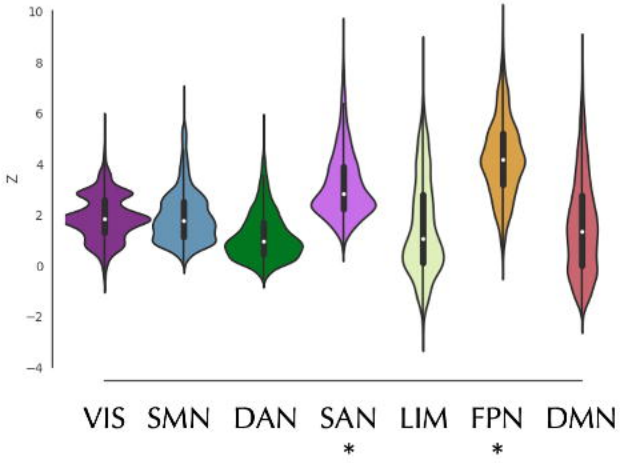

B. Foci distribution across resting-state networks

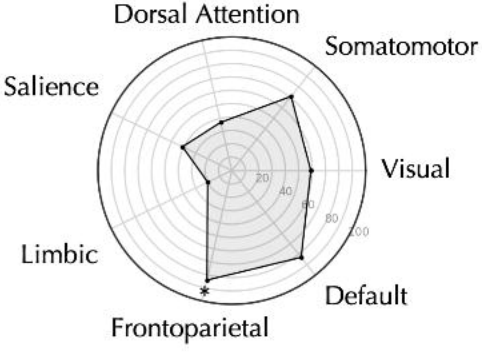

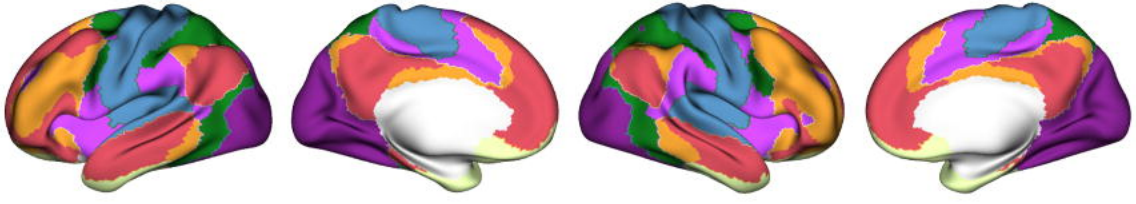

Resting-state networks

A. Receptor/transporter density PET maps

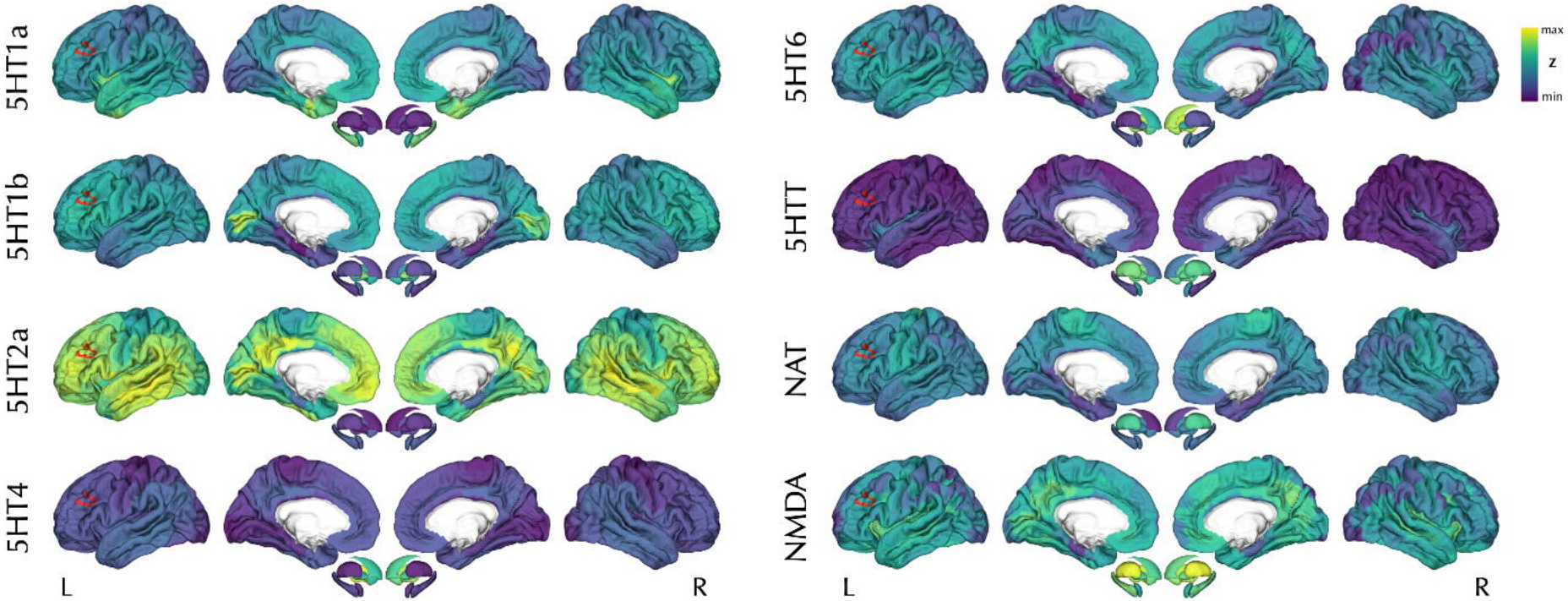

B. Receptor/transporter density in L DLPFC

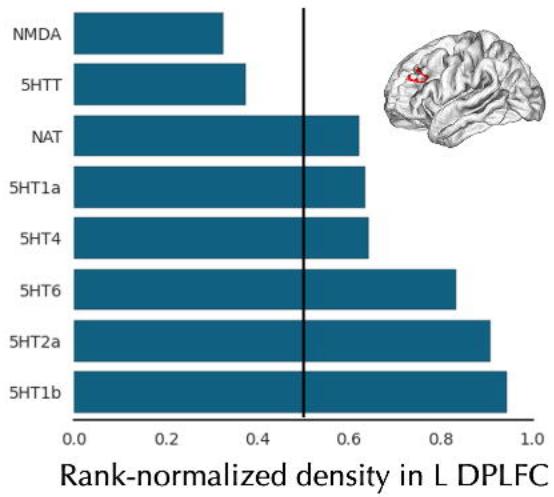
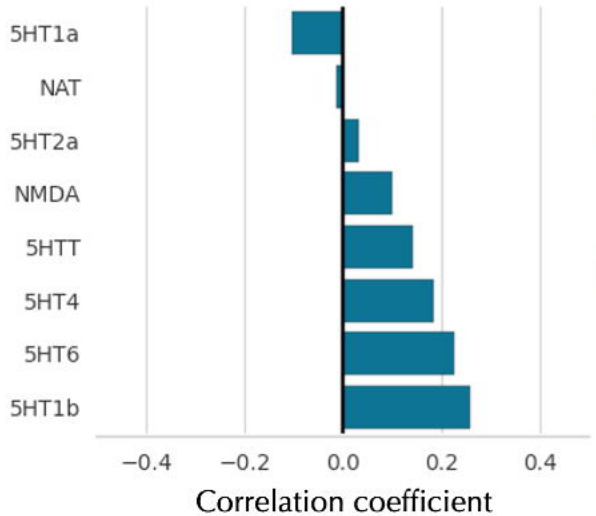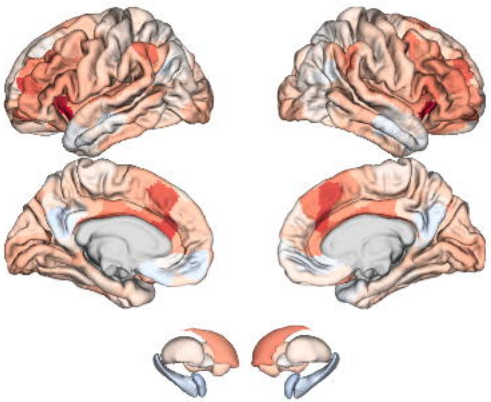
C. Correlation of PET maps with convergent connectivity map